Sequence Stratigraphy as a tool for water resources management in alluvial coastal aquifers: application to the Llobregat delta (Barcelona, Spain)

Desiré Gàmez Torrent

December 2007

CHAPTER 2 : Geochronology of the Pleistocene-Holocene Llobregat delta plain

PhD Thesis

Department of Geotechnical Engineering and Geo-Sciences (ETCG)
Technical University of Catalonia (UPC)

Supervisors:
Dr. J. Antonio Simó Marfà
Dr. Jesús Carrera Ramírez
Tutor:
Daniel Fernández García

Chapter 2

Geochronology of the Pleistocene-Holocene Llobregat delta plain

Deltas are dynamic coastal systems with close links to both land-based fluvial and marine processes. They are of great ecological and economic value throughout the world and are major centers of population and agriculture. One of the major risks in these coastal areas is over-exploitation of groundwater leading to salt-water intrusion in the aquifers. Detailed geological studies can help us to better understand the hydrogeological conceptual model of these systems, which is essential for an appropriate management of water resources.

Reconstruction of the deltaic architecture can be achieved on the basis of process oriented correlation of depositional units. This approach provides guidelines for correlation of stratigraphic bodies and allows matching depositional packages to well established Quaternary sea-level curves. A key factor in the correlation of published sea-level curves is the age of the materials studied. Unfortunately, geological interpretations of cyclic Pleistocene depositional processes are complicated by sediment reworking owing to multiple events (Murray-Wallace et al. 1996; Wehmiller

et al. 1995) due to falling-stages of the sea level and marine transgression (Amorosi, et al. 2004). These processes generated stratigraphic gaps and remobilization of sediment and fauna (Goodfriend and Stanley 1996). Dating is further hindered by the uncertainty of dating due to reworking of sediment, temporary storage of old carbon in delta plains and calibration of radiocarbon dates. Because of these uncertainties some authors (Blockley, Lowe et al. 2004; Goodfriend and Stanley 1996; Stanley 2001) have combined several methods. In this study we will use fauna, age, archaeology, climatology and sedimentological data for the geochronology of the Llobregat delta.

Research in geochronology of Quaternary Mediterranean onshore deltas has been focused on postglacial deposits (late Quaternary), and little has been devoted to Pleistocene with the exception of a few deltas (Amorosi et al., 2001 and 2004). Onshore research has focused on materials deposited after 6500 yr BP, when a deceleration in the rise of sea-level favored the progradation of the deltas (Stanley and Warne 1994). Research issues include the relative influence of autocyclic (i.e., distributary channel avulsion, delta lobe abandonment, human influences, (Barriendos and Martin-Vide 1998; Goy et al., 2003; Liquete et al., 2004; Thorndycraft and Benito 2006a; Thorndycraft and Benito 2006b; Trincardi et al. 2004; Zazo et al. 2003) and allocyclic processes and their influences on the stacking pattern of the holocene parasequences (Diaz et al. 1996; Fernandez-Salas et al. 2003; Lobo et al. 2005b; Somoza et al. 1998;). On the other hand, most of the geochronology of the Pleistocene has focused on submerged deltas (Ariztegui et al. 2000; Cacho et al. 2002; De Kaenel et al. 1999; Thouveny and Berne 2006). As a result, a dichotomy exists between onshore and offshore dates.

The Llobregat delta can be considered paradigmatic in Pleistocene dating. It provides ideal records for dating using a broad range of techniques, while linking the models for onshore to offshore. The aim of this study is thus twofold: a) to provide a Quaternary age model for the Llobregat continental margin based on foraminifers, radiocarbon and amino acid ages and sedimentology, drawing comparisons with global sea level curves; and b) to correlate the sedimentation rate and the sedimentary facies distribution described in onshore cores together with archaeological studies, pollen analysis and palaeofloods in order to evaluate factors that affect the Holocene delta architecture and palaeogeography.

2.1. Onshore geological setting

The Llobregat delta is located south-west of Barcelona in the western Mediterranean (fig. 2.1). The Llobregat River flows north-south from the Pyrenees to the Mediterranean coast, draining an area of 5,045 km^2. It is 163 km in length and has a mean slope of 0.012º. The Llobregat delta plain is confined by the Garraf (SW), Montjuïc (N) and Collserola mountains (NW) and by the Llobregat and Tibidabo faults (fig. 2.1). It covers an area of 95 km^2 and 23 km of shoreline which is influenced by southward longshore currents (about 30 cm/s), low-energy waves and tidal ranges of few centimeters. (Checa et al. 1988). Yearly precipitation in the Llobregat drainage area ranges from 1000 mm in the Pyrenees to less than 600 mm near the coast. The annual flow rate undergoes significant fluctuations (ranging from 270 hm^3/yr to 1347.5 hm^3/yr, between 1912 and 1971), which is typical of Mediterranean regions (Barrera et al. 2005). The palaeoflood record shows a flood frequency pattern linked to climatic oscillations, with increases in the frequency of the Little Ice ages AD 1580-1620, 1760-1800, 1830-1870. The largest flood occurred between AD 1516 and 1642 an estimated minimum discharge of 4680 m^3/s (Barriendos and Martin-Vide 1998; Benito et al. 2005; Llasat, et al. 2005; Thorndycraft et al. 2005a and 2005b; Thorndycraft et al. 2006c).

The Barcelona area consists of two geomorphological units (Cassasas et al 1992), the Upper and Lower Plains, separated by a geomorphological scarp (fig. 2.1). The Upper plain consists of Pleistocene alluvial-fluvial facies dating by U/Th yielding 90 kyr (Julia, R., personal communication) (table 2.1). These deposits rest unconformably on Paleozoic to Pliocene deposits and have a variable thickness (maximum 20m) probably due to filling a palaeorelief (Perea 2006; Ventayol, et al. 2002).

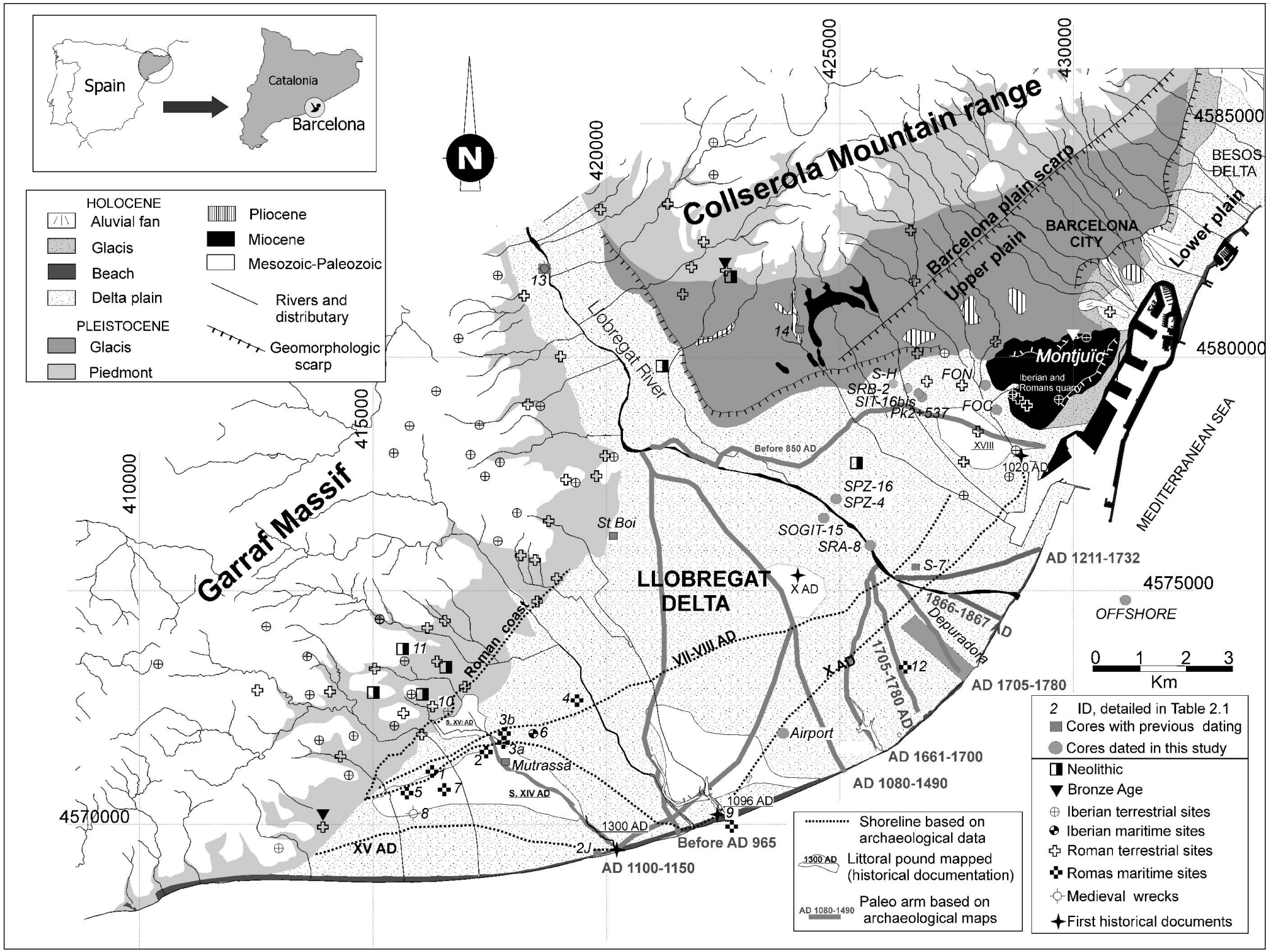

Figure 2.1: Location and geological map of the Llobregat delta and distribution of the cores used in this study. Upper and Lower plain geomorphological units are also shown (modified from Perea, 2006). The figure includes geoarchaeological information from previous studies (table 2.1; Campmany, 2001; Marques, 1984; Izquierdo et al., 1998; Riera et al., 1994).

Table 2.1: Age data from previous studies in the Llobregat delta based on archaeological studies and radioisotope method. The spatial distribution of the data is shown in figure 2.1. BP: Before present; BC: Before Christ; AD: After Christ or Anno Domini.

Methods	ID Fig 2.1	Site Name	Material	Depth (m)	M.A.S.L. (m)	Conventional 14C yr BP	Calendar age	References
ARCHAEOLOGICAL	1	Sorrres I	Shipwreck with wood, amphorae, metals,...	6	-4		I century AD	Izquierdo et al., 1998
	2	Sorres II	Shipwreck & anchorage area with wood, amphoras, dolia, anchors, stone,...	10 / 20 m	- 8 (north) / -18 (south)		IV century BC – II century AD	Izquierdo, 1987: 273-274
	3a	Sorrres IIIa	Shipwreck with wood, amphorae, lead ingots, lead fistulae, dolia, rock mills, 4 iron anchors,...	9	-7		I century AD	Izquierdo et al., 1998
	3b	Sorrres IIIb	Shipwreck with wood, iron anchor, amphorae, pottery,...	9	-7		BC 50 - 25	Izquierdo et al., 1998 & Izquierdo,
	4	Sorres IV	Anchorage area with amphorae, pottery, an iron	Not known	Not known		BC 50-25	Izquierdo, 1987: 278
	5	Sorres V	Anchorage area with amphorae, pottery, a bronze	7	-4 / -5		I century BC	Izquierdo, 1987: 279
	6	Sorres VIII	Shipwreck with wood, amphorae, iron anchors, bronze tools and two Etruscan bronze helmetts				II century BC or later	Izquierdo, 1987: 282. Izquierdo & Solias, 1991: 601-614
	7	Sorres IX	Anchorage area and shipwreck with building marterials (tedulae, locks)	9	-7		I century BC -V century AD	Izquierdo, 1987: 283-284
	8	Sorres X	Merchant ship	3.38	-1,58		AD 1350-1400	Raurich et al., 1992; Izquierdo et al.,
	9	El Remolar	Anchorage or shipwreck with amphorae sand a Nero coin	6 / 20 m	-6 / -20		I century AD	Izquierdo, 1997
	10	"La Roca" Iberian	Fossil dunes of a Iberian period	2	0,5		Iberian times	Izquierdo, oral communication
	11	Mines Can Tintorer	Turquoise & iron mining complex	Surface / -25	40 / 60		BC 3400 –AD 100	Riera, 1994
	12	La Ricarda	Anchorage with amphoras	20 / 25	-18 /-23		I century BC	Izquierdo 1997 and oral
	13	Garrigosa	Anchorage & wharf	8.5	6.5		I century BC	Gimenez et al.1994 , unpublished
		Garrigosa	Mill	1.6	13.4		XVI century AD	Gimenez et al.1994 , unpublished
RADIOCARBON		2J	Peat	53	-50.1	10900±140	BC 8950±140	Marques, 1984
		S7'	Scattered carbon	34.1	-28.1	2300±1200		Manzano et al., 1986-1987
		St Boi	Peat	7.1	-3.9?	3185±29		Riera, unpublished
		Mutrassa	Peat	1.9	13.1	1248±24	VIII century AD	Riera et al., 1994a
	13	Garrigosa	Peat (marsh top)	7.3	7.7	1200		Santi Riera, personal communication
		Garrigosa	Peat (marsh base)	7.9	7.1	2020		Santi Riera, personal communication
		Garrigosa	Trees: Quercus s.p (transport)	12	3	4680±60	cal BC 3640-335	Gimenez et al.1994 , unpublished
		Garrigosa	Trees: Quercus s.p (transport)	12	3	1840±70	cal AD 60-350	Gimenez et al.1994 , unpublished
		Garrigosa	Trees: Quercus s.p (in situ) and pottery	12	3	4710±60	cal BC 3630-3360	Gimenez et al.1994 , unpublished
DATING (U/Th)	14	Barcelona tricicle	Paleosoils in upper plain unit	middle unit		aprox 90000		Ramon Julia, personal communication

This study focuses on the Lower plain, previously studied by numerous authors (Almera 1891; Llopis 1942; Llopis 1946; Solé-Sabaris et al. 1957; Solé-Sabarís et al., 1963). The "Comissaria d'Aigües del Pirineu Oriental" was the first to describe the main hydrogeological units MOP (1966), and Marques (1984) reported two quaternary detritical complexes: a Pleistocene Lower Detritical Complex (LDC) and a Holocene Deltaic Complex or Upper Detritical Complex (UDC) (fig. 2.2). Offshore studies documented four deltaic units (Medialdea et al. 1986 and 1989). The three older offshore deltaic units correlate with the LDC and the modern seismic unit with the Upper Detritical Complex (UDC) (Simó et al., 2005).

The LDC consists of fluvial gravels interbedded with yellow and red clays that grade to offshore clays seaward (Marques, 1984). Recent studies by Simó et al. (2005) discussed in detail in Chapter 3 have recognized a minimum of three fault-controlled palaeochannels (figs. 2.2 and 2.3) separating nearshore to delta plain deposits. The palaeochannels define fining upward depositional sequences which overlie an erosional surface and underlie a planar surface. The two older palaeochannels with incisions at the bottom and flat surface on top are capped by fine sediments (Rw, fig 2.3). However, the upper palaeochannel is postdated by the Deltaic complex (UDC). The Llobregat River and streams from the Garraf, Montjuïc, and Collserola mountains fed these palaeochannels, which in turn fed the offshore deltas (Medialdea et al., 1986 and 1989; Simó et al 2005). Manzano (1993) interpreted these deposits (unit-e and unit-f) as 18,000–10,500 yr BP in age (Würm IV) while Marques (1984) recognized three transgressive-regressive cycles deposited during the Flandrian interglacial (fig. 2.2).

The UDC is composed of four lithofacies, from bottom to top, transgressive sands (unit d), prodelta silts deposited in a shallow to deep shelf (unit c), delta front sands and silts (unit b), and an uppermost unit consisting of delta plain gravels and sands, flood plain fine sands, silts, red clays and dark-organic silts (unit a, fig. 2.2) (Marques, 1984; Manzano, 1986, 1993). The thickness of the UDC attains 60 m in the center of the delta, thinning out towards the margins (figs. 2.2 and 2.3). Ten radiocarbon dates were reported from UDC units (fig. 2.1, table 2.1), suggesting that

unit-d is 10,500 yr BP, unit-c 9,000-8,000 yr BP, and unit a and b younger than 6000 yr BP (Manzano et al., 1986-1987; Manzano, 1993; Marques, 1984; Monaco et al., 1972) (fig. 2.2). Checa et al (1988) reported that the progradation (unit c) commenced at 6000 yr BP. Earlier geoarchaeology studies (table 2.1) in UDC deposits show the reconstruction of the shoreline evolution from Roman times to the present (Marques, 1984; Raurich et al., 1992; Riera et al., 1994; Izquierdo et al., 1985, 1987a, 1987b, 1987c, 1992, 1997; 1998, and 2001), which will be used for the evolution of the Holocene delta plain (see section 2.4.1).

The Llobregat stratigraphic architecture discussed in Chapter 3 is supported by the palaeontology and ages displayed in this Chapter. In Chapter 3, the integration of coastal plain sediment cores with offshore seismic records provides an overall picture of the stratigraphic architecture of the continental margin composed of progradational wedge deposits that increase in thickness seawards (fig. 2.11) (Chapter 3 and Appendix IV). The onshore-offshore correlation is based on the identification of fluvial incisions in the delta plain (fig. 2.3) and the erosional truncations offshore, and on planar surfaces throughout the onshore-offshore domain. Three regional erosional and planar surfaces were identified and interpreted as a Sequence boundary (SB III, II and I, figs. 2.2 and 2.3) and maximum flooding surface (mfs, fig. 2.2), respectively. These sequence boundaries (SB I, II and III) establish the boundary of four Quaternary depositional sequences in the Llobregat delta (from base to top DS IV, III, II and I, fig. 2.3 and 2.11) and can be related to major sea-level falls (figs. 2.2 and 2.4). We replace the old nomenclature UDC and LDC by the Depositional Sequence nomenclature.

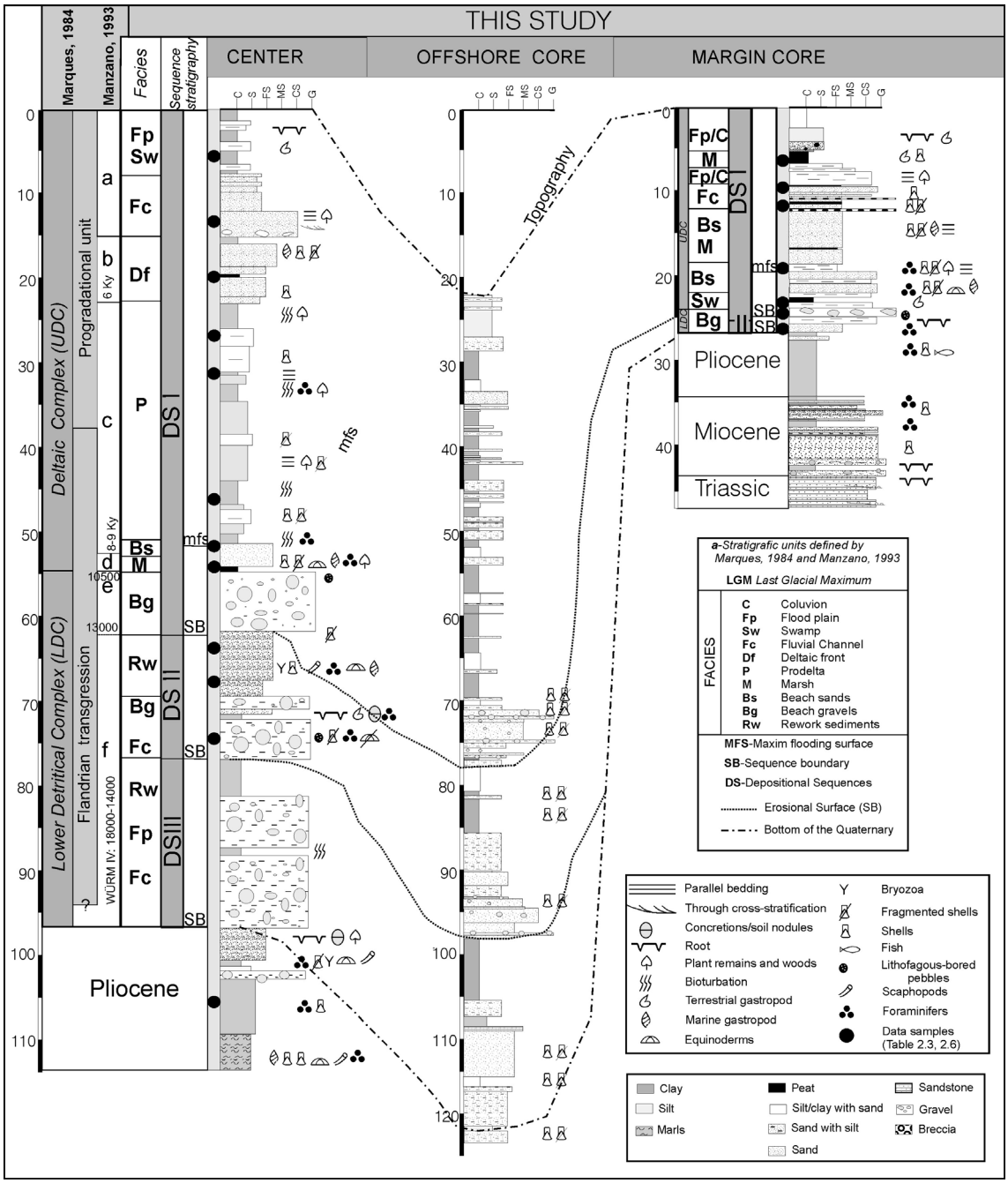

Figure 2.2: Representative stratigraphic sections and vertical facies distribution in the center of the delta and eastern margin of Llobregat in delta plain and offshore, showing a schematic correlation of the stratigraphic units. The stratigraphic units and geochronology information from previous studies is compared with the new information provided in this study. The position of the amino acid racemization and radiocarbon ages is approximated within the facies dated (for a precise location of the cores, see fig. 2.4).

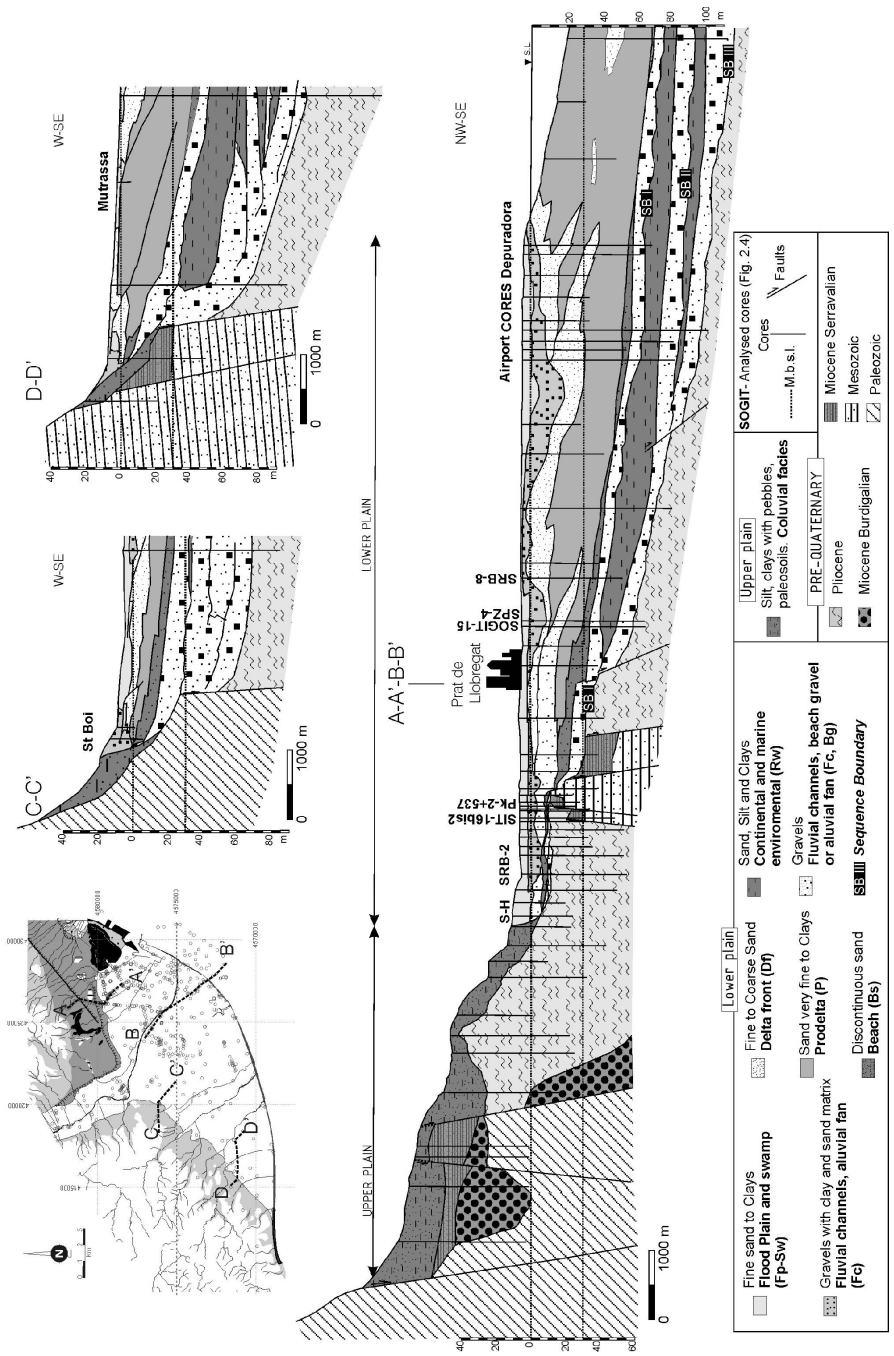

Figure 2.3: Dip cross sections of the Llobregat delta deposits after core-descriptions and dating and palaeontology data presented in this study (more details in Appendix III). Three regional erosional surfaces (SB) recognized in Pleistocene deposits are displayed. The datum of the cores is the current sea level. The name of the cores used in this study is also included (for detail core description see fig. 2.4). The cross section is located in the upper left corner (Perea et al. 2006).

2.2. Methods

This study contains information from over 618 onshore and 30 offshore cores; 560 cores have been previously described and 88 are new descriptions. Eleven cores based on their data quality, spatial distribution, and continuous record through the Quaternary complex and basement with depths ranging between 50 to 140 meters was selected for dating (figs. 2.1 and 2.4). A total of seventy one samples were analyzed for dating (radiocarbon and amino acid racemization) and foraminiferal analyses.

2.2.1. Foraminifers identification

Thirty six samples were selected for foraminiferal identification from the Depositional Sequence I, II, III and probably IV, and basement (figs. 2.4 and 2.5). The samples were disaggregated using water and 10 gr. of weight sediments, sieved through 0.5; 0.2 and 0.062 mm sizes and hand picked. This kind of treatment allows us to preserve the majority of the most fragile tests and to retain the smaller specimens, not only the young ones. We did not use carbon tetrachloride to extract the foraminifers from the sediment because the specimens were too heavy to float.

For samples from SPZ-4 between 47 to 68 m, we quantified the number of individuals of benthic or planktonic foraminifers to obtain a vertical variation of the proximal and distal facies (fig. 2.6). The identification of the planktonic and benthonic foraminifers and the interpretation of the age indicators and the sedimentary environmental are based on the following studies: Amorosi et al. (2004), Bellotti et al. (1995), Magne (1978), Murray (1991), Usera et al. (1991), and Usera et al. (2002). Data obtained by this method are shown in tables 2.2 a, b and c.

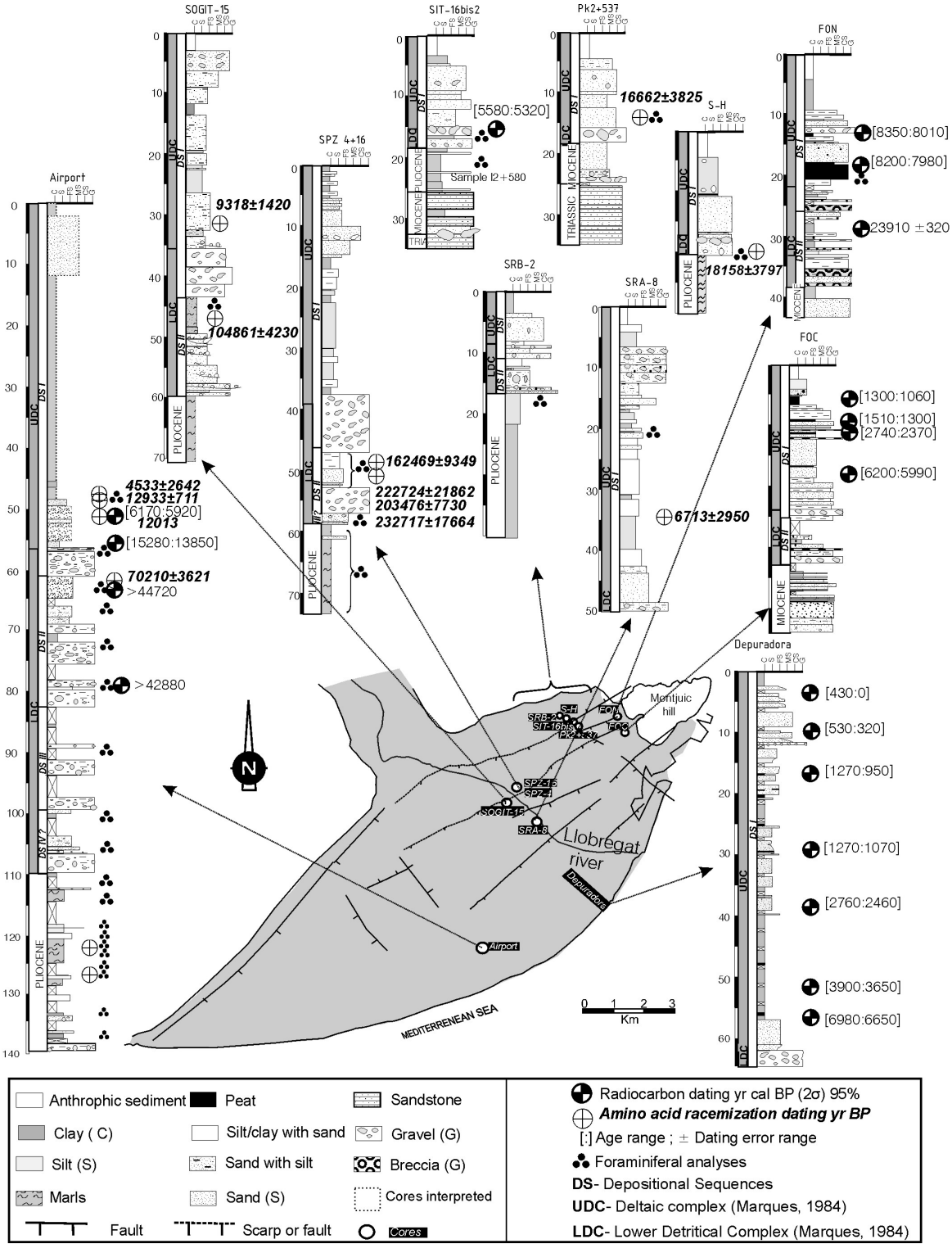

Figure 2.4: Stratigraphic description of the cores sampled for dating (radiocarbon and aspartic acid racemization) and palaeontological analyses in the Llobregat delta. Note that the core I2+580 is not represented because it is similar to the SIT-16bis core and is located at a distance of 25 m. DS: Depositional Sequence

2.2.2. ^{14}C dating

Seventeen samples from the Depositional Sequence I and three from Depositional Sequence II were analyzed for radiocarbon dating (fig. 2.4). Shells and organic matter were dated by AMS (Accelerator Mass Spectrometry) and conventional radiocarbon methods by Beta Analytic Inc., Florida (USA). The $^{13}C/^{12}C$ ratio is expressed in terms of δ per mil (‰) referred to PDB (Pee Dee Belemite). The ages have been corrected for the marine reservoir effect by subtracting 430±50 years (Stuiver et al., 1986; Stuiver et al., 1993). Subsequently, the results were calibrated using the INTCAL program 98 (Stuiver et al., 1998), with the exception of the sample FON-28.7, which was performed with CAL_PAL program and calibration dataset CalPal2005_SFCP (Weninger et al., May 2006). The calibrated age is expressed as a standard deviation 2σ (95% confidence intervals) (Stuiver et al., 1998). The data obtained from this method are shown in table 2.3.

2.2.3. Sediment Accumulation Rates

Sedimentation rates for Depositional Sequence I was calculated from radiocarbon ages (mean yr cal BP, table 2.3) on Depuradora, Airport and FOC cores (fig. 2.4). These cores were selected because they represent a continuous dating record located in the center of the delta (Depuradora and Airport) and the margin of the delta (FOC) (fig. 2.4). The mean of the calibrated radiocarbon ages in the stratigraphic column (yr cal BP 2σ, table 2.3) and the accumulated thickness yielded more accurate sedimentation rates (eq.1, 2 and 3, table 2.7). The minimum and maximum errors in the sedimentation rate, using the error associated with the ages, was also calculated (eq.1, 2 and 3, table 2.7).

$sr = \frac{(d_2 - d_1)}{(\bar{t}_2 - \bar{t}_1)} \times K$ Eq. 1	$\varepsilon_{\max} = \frac{(d_2 - d_1)}{(\bar{t}_2 - \xi_2) - (\bar{t}_1 + \xi_1)} \times K$ Eq. 2
	$\varepsilon_{\min} = \frac{(d_2 - d_1)}{(\bar{t}_2 + \xi_2) - (\bar{t}_1 - \xi_1)} \times K$ Eq. 3

Where *sr* is the sedimentation rate (mm/yr), *d* is depth (m), $\bar{t}$ is mean radiocarbon age (yr cal BP) from table 2.3, ξ is the age error range and *K* is 1000 for conversion into depth units. The maximum and minimum sedimentation rate errors were chosen from the four error combinations (ε_{max} and ε_{min}). The results of the calculation are shown in table 2.7.

The sedimentation rate curve was plotted using cores from the center of the delta ("Depuradora" and Airport cores) owing to higher record thickness. Based on the results shown in table 2.7, we plotted sedimentation rate values with minimum and maximum errors.

2.2.4. Aspartic acid racemization dating

Amino Acid Racemization method (AAR) is especially useful for the age range beyond the range of ^{14}C and U/Th methods as well as Holocene materials (Goodfriend, 1991; Goodfriend, 1992; Goodfriend et al., 1992; Goodfriend et al., 1995).

Of the different dating methods, amino acid racemization can be applied to a large number of materials including mollusk and ostracod shells. The method relies on the fact that in most living beings amino acids are laevorotatory (L-amino acids). When an organism dies there is a progressive transformation of *L*-enantiomens into *D*-enantiomers (dextrorotatory) in a process called racemization. When the *D*/*L* ratio approaches 1, the process is almost in equilibrium and the racemic state is attained, marking the method range.

Thirteen samples were analyzed using amino acid racemization at the Biomolecular Stratigraphy Laboratory of Madrid (Universidad Politécnica de Madrid, Spain) (fig. 2.4). Between one and nine ostracod valves were extracted from the sediment samples. Although the use of monogeneric samples reduces taxonomically controlled variability in *D*/*L* ratios (Murray-Wallace, 1995; Murray-Wallace et al., 1995), we used ostracod valves from different genera owing to low numbers. In the laboratory, shells were carefully sonicated and cleaned with H_2O_2 to remove sediment and organic matter. Amino acid concentrations and racemization ratios were quantified using an HPLC following an established protocol (Kaufman et al., 1998;

Kaufman, 2000). Palaeoenvironmental interpretation were interpreted (Guillaume et al., 1985). The data obtained from this method are shown in table 2.6.

2.3. Results

2.3.1. Foraminifers

Foraminiferal results are shown in tables 2.2a, 2.2b and 2.2c, and figs. 2.5 and 2.6 Planktonic foraminiferal species providing age are *Globigerinoides sicanus* (Langhian and Serravallian), *Globigerinoides obliquus extremus* (Middle Pliocene), and *Truncorotalia truncatulinoides* or *Truncorotalia crassaformis* and *Globigerinoides ruber* acnezone (Quaternary, fig. 2.5). The most common benthonic foraminifers are *Aubignyna mariei* and *Aubignyna prelucida* indicative of Upper Pliocene and of Quaternary ages, respectively (fig. 2.5). Miocene and Pliocene foraminiferal species are often found together in Quaternary samples suggesting abundant reworking. Overall, the foraminifers observed in this study present a high grade of poor shell preservation and are often mineralized.

Water temperatures were interpreted for most of the Llobregat samples (table 2.8). Interpretations are based on the overall size of individuals and especially in the presence of the temperature indicator *Globigerinoides sacculifer*.

Foraminifera associations from deeper to shallower environments were described as follows.

a) Open marine shelf environments (Circalittoral environment)

High diversity of foraminifera specimens. Dominant assemblage of planktonic foraminifers indicative of open marine, inner shelf subenvironment, such as *Globigerinoides sacculifer*, *Globigerinoides obliquus extremus* and *Globigerinoides ruber*. Benthonic foraminifers *Lenticulina* sp., *Uvigerina peregrina* and *Globobulimina pyrula* are found particularly in Pliocene deposits.

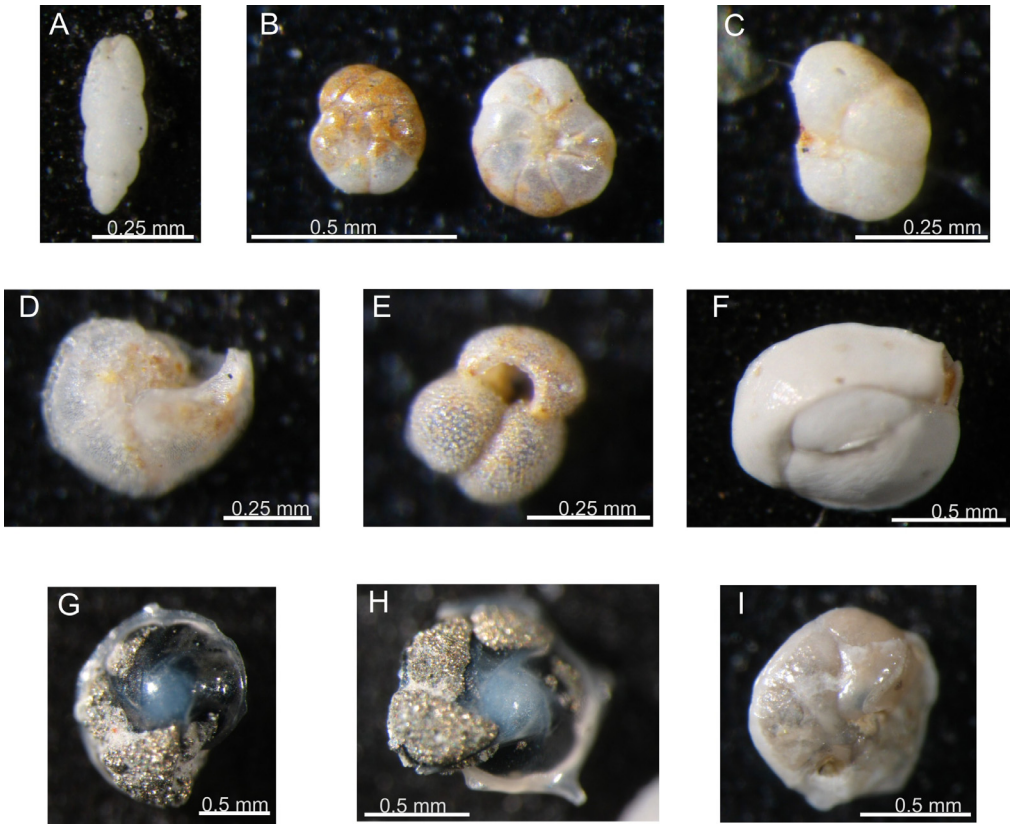

Figure 2.5: Foraminiferal identification of samples in this study. We recognize a restricted sedimentary enviroment: **A**. SPZ 4 -58.4: Bulimina elongata (D'Orbigny); Age foraminifers: Pliocene foraminifers: **B**. SPZ 4-49.2:Aubignyna mariei (Margerel), Quaternary foraminifers: **C**. SPZ 4-49.98: Aubignyna perlucida (Heron-Allen & Earland), **D**. SPZ 4-49.92:Truncorotalia truncatulinoides (D'Orbigny) **E**. SPZ 4-49.98:Globigerinoides ruber (D'Orbigny), and taphonomic processes and diagenesis: D.SPZ 4-49.92:Truncorotalia truncatulinoides (D'Orbigny), broken, **F**. SIT 16 bis2-17: Masselina secans (D'Orbigny), broken, **G**, **H**: I2+580-31: Lenticulina calcar (Linné), pyrititzation, **I**: SPZ 4-49.98: Eponides repandus (Fichtell & Moll), broken and refill of sediments.

b) Nearshore environment (Infralittoral environmental)

A relative decrease in planktonic foraminiferal species is observed whereas benthonic foraminifers are more abundant. The dominant species are *Elphidium crispum*, *Nonion comune*, *Ammonia beccarii inflata*, *Ammonia beccarii punctatogranosa*, *Quinqueloculina sp*. and *Lobatula lobatula.* Agglutinated foraminifers such as *Textularia* spp were also reported.

The existence of a highly reworked foraminiferal species from the Miocene and the Pliocene in the Quaternary units together with resedimentated foraminifers consisting of deep and shallow-water species, and broken shells are interpreted as a beach ridge sub-environment (Upper/ Lower shoreface) or beach barrier sand and

gravels. We interpreted as a gravel beach subenvironment in the Airport 78.1 and SPZ-4 47.8 samples (fig. 2.4).

c) Lagoon and marsh (brackish water environment)

Different subenvironments were distinguished in the brackish water environment:

-Lagoon sub-environments, which are very sensitive to temperature and salinity, are recognized, presenting low frequency of benthonic foraminifers. The dominant species are *Ammonia beccarii tepida*, *Elphidium excavatum*, *Aubignyna prelucida* and *Aubignyna mariei* (fig. 2.5). Restricted areas with anoxic conditions are identified by the presence of B*ulimina elongata* (fig. 2.5) and *Bolovina pseudopunctata*. The foraminiferal shells underwent dissolution and later pyrite precipitation. This association is found particularly in Pliocene deposits (fig. 2.5).

- Subenvironments of washover are composed of silt lamination and sandy silt, and mixed fauna indicative of marine and brackish water. They were formed from the rupture of the beach barrier by storm processes, with a subsequent settling out in the lagoon. Foraminiferal shells are poorly preserved, often partially dissolved, broken or iron oxidized.

- The Airport 54.86, 99.1 and 105.2 samples were interpreted as marsh organic-rich clays characterized by the lowest diversity of benthic foraminifera species. The species *Ammonia beccarii tepida*, *Elphidium excavatum*, *Haynesina germanica* were identified but were few in number.

d) Swamp (freshwater environment)

No foraminiferal specimens were found in the Airport 88.1 and Airport 135.45 samples (fig. 2.4). These were interpreted as flood plain, described as red clays which showed bioturbation and plant remains. Resedimented foraminifers with poor preservation and iron oxide crust were interpreted in the Airport 71.8 sample (fig. 2.4). The SRA8-22.4 and FON-21.2 samples were interpreted as swamp environments because of the high percentage of plant remains, gasterpopoda and shells and the absence of ostracod.

Sediments described between palaeochannels in DS II and III (Rw facies, fig 2.3) are interpreted as sediments deposited from continental to marine environmental, with a high degree of reworking. These sediments are known as multicolored fine-grained facies association (Chapter 3).

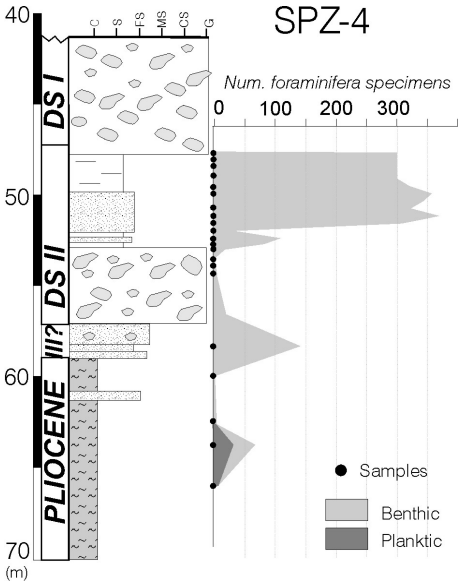

Figure 2.6: Variation in the number of benthonic and planktonic foraminifera specimens counted in SPZ-4 core (40-70 m depth interval). Note that the majority of foraminifers show evidence of reworking. See detail record SPZ-4 core in fig. 2.4.

Table 2.2a: Foraminiferal results from the SPZ-4 core. Sample location along the core is shown in figure 2.4. The interpretation of the foraminifera associations and taphonomic processes is given in table 2.8. DS: Depositional Sequence, PL: Pliocene.

Core	SPZ-4												
Depth	47.8	48.6	49.2	49.63	50.0	50.8	51.59	52	52.44	52.8	58.4	63.8	68.2
Depositional Sequences	DS I	DS II										PI	
Benthic Forams													
Adelosina laevigata				x									
Ammonia beccarii	x	x	x	x	x	x	x				x	x	x
Ammonia beccarii puntatogranosa	x	x	x		x	x	x	cf	cf	cf			
Ammonia beccarii tepida											x		
Aubignyna mariei			x										
Aubignyna perlucida		x	x	x	x	x					x		
Bolivina pseudopunctata											x		x
Bulimina aculeata		x	x		x		x						
Bulimina elongata											x		x
Bulimina marginata			x										
Elphidium advenum	x	x	x		x	x	x						
Elphidium complanatum					x								
Elphidium crispum	x	x	x	x	x	x	x	cf	cf	cf			
Elphidium excavatum		x	x	x	x	x							
Elphidium granossum													x
Fursenkoina schreiberiana			x										
Haynesina germanica	x		x				x						
Lenticulina sp.											x		
Lobatula lobatula					x								
Massilina secans	x												
Nonion commune	x	x	x	x	x	x					x		x
Nonionella stella	x	x	x		x								
Quinqueloculina seminula	x												
Planctonic Forams													
Globigerina bulloides					x								
Globigerinella aequilateralis					x								
Globigerinoides ruber		x			x								
Globigerinoides sacculifer			x										
Globigerinoides sp.												x	x
Truncorotalia crassaformis			x	x		x							
Truncorotalia truncatulinoides		x	x										

Table 2.2b: Foraminiferal results from the Airport core. Sample location along the core is shown in figure 2.4. The interpretation of the foraminifera associations and taphonomic processes is given in table 2.8. DS: Depositional Sequence, PL: Pliocene.

Core	Airport										
Depth	48.92	48.98	49.11	60.9	65.68	71.8	78.6	99.1	103.5	105.2	118.9	126.4
Depositional Sequences	DS I			DS II				DS III	DSIV?		Pl	
Benthic Forams												
Adelosina colomi			x									
Adelosina laevigata			x									x
Adelosina pulchella	x		x									x
Ammonia beccarii						x	x	x	x	x	x	x
Ammonia beccarii inflata	x	x	x							x		x
Amphistegina hauerina									x		x	
Amphycorina sp.												x
Asterigenata mamilla					x					x		
Aubignyna mariei					x				x			
Bolivina sp.											x	
Bolivina dilatata												x
Brizalina aenariensis					x							
Bulimina elongata					x			x	x			x
Bulimina marginata						x		x	x	x		x
Bulimina puntata					x							
Cabicidoides sp.										x		
Cancris auricula			x						x			x
Cassidulina laevigata									x			
Cibicidella variabilis				x								
Dorothia gibbosa												x
Elphidium aculeatum				x								
Elphidium advenum									x			x
Elphidium complanatum				x				x	x			
Elphidium crispum	x	x	x	x			x	x	x	x	x	x
Elphidium excavatum			x								x	
Elphidium macellum			**cf**						x		x	
Elphidium sp.					x							
Fursenkoina schreiberiana					x					x		x
Globocassidulina oblonga	x								x	x	x	
Guttulina communis							x					
Hanzawaia boueana			x		x					x		
Haynesina germanica					x							
Hopkinsina bononiensis						x						
Lenticulina calcar					x							
Lobatula lobatula		x	x	x	x			x		x	x	x
Melonis pompilioides	x	x										
Miliolinella circularis												x
Neoconorbina terquemi				x								
Nonion commune	x	x	x		x	x	x	x	x	x		x
Nonionella stella												x
Oolina sp.											x	
Planorbulina mediterranensis			x	x								
Pyrgo sp.		x										
Quinqueloculina sp.				x								
Quinqueloculina bicornis												x
Quinqueloculina lamarckiana				x								
Quinqueloculina lata												x
Quinqueloculina oblonga												x
Quinqueloculina quadrata												x
Quinqueloculina seminula	x	x	x									x
Quinqueloculina vulgaris												x
Reussella spinulosa												x
Rosalina bradyi				x								
Sigmoilina grata				x								
Sigmoilopsis schlumbergeri	x											
Spiroloculina depressa			x									x
Siphotexturalia sp.												x
Textularia agglutinans			x									
Textularia gramen			x									
Textularia sagitula	x	x	x		x					x		x
Triloculina trigonula		x	x	x								x
Valvulineria bradyana	x	x	x			x						x
Planctonic Forams												
Globigerina bulloides	x	x	x									x
Globigerina falconensis			x									
Globigerinella aequilateralis		x										
Globigerinoides obliquus					x					x		
Globigerinoides ruber		x	x									**x?**
Globigerinoides sacculifer			x		x							
Globigerinoides sp.	x	x										x
Orbulina universa	x		x									

Table 2.2c: Foraminiferal results from different cores. Sample location along the core is shown in figure 2.4. The interpretation of the foraminiferal associations and taphonomic processes is given in table 2.8. DS: Depositional Sequence, PL: Pliocene

Cores	SPZ-16	SRB-2	SOGIT-15	I2+580	pk2+537	S-H	SIT-16 bis2
Depth	50.3	18.2	45.35	31	15.3	19.4	17
Depositional Sequences	DS II	Pl	DS II	Pl		DS I	
Benthic Forams							
Ammonia beccarii	x	x	x		x	x	
Ammonia beccarii inflata							x
Ammonia beccarii puntatogranosa	x						x
Amphycorina scalaris				x			
Aubignyna mariei	x						
Aubignyna perlucida	x		x				
Bigenerina nodosaria		x					
Bolivina arta		x					
Brizalina alata		x		x			
Bulimina aculeata			x				
Bulimina elongata		x					
Bulimina marginata		x	x	x			
Cancris auricula		x					
Cassidulina laevigata		x					
Cibicidoides kullembergi		x					
Cibicidella variabilis					x		
Chrysalogonium sp.		x					
Dentalina sp.							x
Dorothia brevis		x					
Dorothia gibbosa		x					
Elphidium aculeatum			x			x	
Elphidium advenum			x				
Elphidium complanatum	x		x		x		
Elphidium crispum	x		x		x	x	x
Elphidium excavatum	x						
Elphidium granossum			x				
Eponides repandus							x
Fursenkoina schreiberiana		x	x				
Globobulimina pyrula		x		x			x
Heterolepa dertonensis		x		x			x
Heterolepa floridana				x			x
Heterolepa perlucida		x					
Hopkinsina bononiensis		x	x				
Lenticulina calcar		x		x			x
Lenticulina cultrata		x					
Lenticulina vortex		x					
Lobatula lobatula		x			x	x	
Marginulina costata		x		x			
Martinottiella communis		x					
Massilina secans					x		x
Melonis barleeanum			x				
Melonis pompilioides		x		x			
Miliolinella circularis					x		
Neoeponides schreibersii		x					
Nodosaria acuminata		x					
Nodosaria sp.							x
Nonion commune	x	x	x	x			x
Nonionella stella			x				
Orthomorphina tenuicostata		x					
Planorbulina mediterranensis					x		
Pullenia bulloides		x					
Quinqueloculina agglutinans					x		
Quinqueloculina oblonga					x	x	
Quinqueloculina rugosa							x
Quinqueloculina sp.						x	
Reussella spinulosa	x	x	x				
Rosalina bradyi						x	
Sphaeroidina bulloides		x					
Textularia gramen		x					
Textularia sagitula		x		x			
Triloculina trigonula					x		
Uvigerina peregrina		x		x			
Valvulineria bradyana	x	x	x	x			x
Plantonic Forams							
Globigerina apertura		x		x			
Globigerina bulloides	x	x	x	x			
Globigerina falconensis			x				
Globigerinella aequilateralis				x			x
Globigerinoides obliquus	x	x		x			
Globigerinoides ruber	x				x		
Globigerinoides sacculifer	x	x					
Globigerinoides sicanus		x					
Globigerinoides trilobus							x?
Globulina gibba					x		
Hastigerina pelagica		x					
Orbulina universa		x		x			
Truncorotalia crassaformis	x						
Truncorotalia inflata			x				
Truncorotalia truncatulinoides			x				
Turborotalia quinqueloba			x				

2.3.2. ^{14}C dating

The samples from the five cores present progressively older ages with core depth (table 2.3 and fig. 2.4). The radiocarbon results in Depositional Sequence I is consistent with the stratigraphic succession. Unit d, interpreted from foraminiferal analyses as beach sand, marsh and swamp shows dates between 14,565 and 5,450 yr cal BP (figs. 2.2 and 2.4, table 2.3). The marsh and swamp facies yield dates between 14,565±715 yr cal BP in the center of the delta (Airport-54.86, fig. 2.4, table 2.3) to 8,090±110 yr cal BP in the eastern margin (FON-18, fig. 2.4, table 2.3) and are in agreement with earlier results (Marques, 1984, table 2.1). The beach sand facies, capping unit d, are dated at 6,045±125 yr cal BP (center of the delta, Airport-49.11, fig. 2.4, table 2.3) and 6,095±105 and 5,450±130 yr cal BP (margin, fig. 2.4, table 2.3). The prodelta facies interbedded with marsh deposits (unit- c, fig. 2.2) sampled in the center of the delta yielded an age of 6,815±165 yr cal BP at the base to 2,610±150 yr cal BP towards the top of the unit. Towards the eastern margin, the prodelta facies correlate with marsh facies with ages of 2,555±185 yr cal BP (fig. 2.4, table 2.3). These ages agree with earlier dates (Manzano 1986, fig. 2.1, table 2.1). Results for delta front facies (unit-b, fig. 2.2) indicate ages in the center of the delta between 1,170±100 at the base of the unit and 1,110±160 yr cal BP at the top (fig. 2.4, table 2.3). Towards the eastern margin they correlate with marsh facies dated at 1,405±105 and 1,180±120 yr cal BP (fig. 2.4, table 2.3) and in the western margin, with marsh facies was dated at 3,185±29 yr BP (Riera et al, 1994a, table 2.1). The flood plain facies at the top of the Depositional Sequence I (unit a) yielded an age of 425±105 to 215±215 yr cal BP in the center of the delta (fig. 2.4, table 2.3).

All attempts to date Depositional Sequence II using ^{14}C methods (table 2.3, fig. 2.4) indicated ages older than the effective dating range of the radiocarbon method. Only one sample collected from the flood plain in the FON core in the margin (FON-28.7, fig. 2.4, table 2.3,) gave an age of 23,910±320 yr cal BP.

Table 2.3: Results of 14C analysis on samples from the Llobregat Delta. (*) corrected for local reservoir effect. The facies interpretation (see nomenclature in figure 2.3) and the corresponding depositional sequence (DS) are also included in the table. Bold mean cal BP will be used in table 2.7. BP: Before present; BC: Before Christ; AD: After Christ or Anno Domini; Cal: Calibrated year. Nomenclature used in the Quaternary Llobregat sediments: Fp (Flood plain); Df (Delta front); P (Prodelta); Bs (Beach sand); M (Marsh); Sw (Swamp); Bg (Beach gravel); Bs (Beach sand) and Rw (Multicolored fine-grained facies association). DS (Depositional Sequence).

Core	Depth (m)	M.B.S.L. (m)	Lab code	Material	Method	$^{13}C/^{12}C$ (o/oo)	Conventional ^{14}C yr BP	2σ calibrated age range (Cal. BP)	Calendar Age (BC/AD)	Mean Cal.(BP)	Facies	DS
Depuradora	**4.2**	1.9	Beta-192479	charred material	Standard	-25.9	190±70	430-0	AD 1,520-1,950	**215±215**	Fp	I
Depuradora	**9.6**	7.3	Beta-192480	wood	Standard	-25.9	420±50	530-320	AD 1,420-1,630	**425±105**		
Depuradora	**17.7**	15.4	Beta-192481	peat	Standard	-26.4	1,180±70	1,270-950	AD 680-1,000	**1,110±160**	Df	
Depuradora	**28.95**	26.65	Beta-192482	concentration of fibrous organics	Standard	-25.3	1,250±40	1,270-1,070	AD 680-880	**1,170±100**		
FOC	**6.6**	0.2	Beta-196459	peat	Standard	-26.9	1,270±60	1,300-1,060	AD 650-890	**1,180±120**	M	
FOC	7.7	0.9	Beta-196458	peat	Standard	-27.7	1,270±60	1,300-1,060	AD 650-890	1,180±120		
FOC	9.5	2.7	Beta-196460	peat	Standard	-29.2	1,490±50	1,510-1,300	AD 440-650	1,405±105		
FOC	11.6	4.8	Beta-196461	organic sediment	AMS	-26.9	2,500±40	2,740-2,370	BC 790-420	2,555±185		
Depuradora	**38.5**	36.2	Beta-192483	charred material	AMS	-26	2,540±50	2,760-2460	BC 810-520	**2,610±150**	P	
Depuradora	**51.8**	49.5	Beta-192484	wood	AMS	-28.1	3,510±50	3,900-3,650	BC 1,950-1,700	**3,775±125**		
SIT-16 bis2	15	8.2	Beta-217689	shell	Standard	2.1	5,100 ±50	5,580 - 5,320	BC 3,620-3,370	5,450±130	Bs	
FOC	**18.3**	11.5	Beta-196464	shell	AMS	-0.2	5,710±40	6,200-5,990	BC 4,250-4,040	**6,095±105**		
Airport	**49.11**	47.81	Beta-201546	shell	AMS	0.7	5,650±50	6,170-5,920	BC 4,220-3,970	**6,045±125**		
Depuradora	**56.4**	54.1	Beta-192485	organic sediment	Standard	-26.2	5,970±70	6,980-6,650	BC 5,030-4,700	**6,815±165**	P	
FON	18	9.2	Beta-196463	peat	Standard	-27.2	7,310±60	8,200-7,980	BC 6,250-6,030	8,090±110	Sw	
FON	13.27	4.47	Beta-196462	organic sediment	Standard	-24.4	7,370±70	8,350-8,010	BC 6,400-6,060	8,180±170		
Airport	**54.86**	53.56	Beta-201547	organic sediment	AMS	-26.3	12,180±60	15,280-13,850	BC 13,330-11,900	**14,565±715**	M	
FON	28.7	19.9	Beta-201548	organic sediment	AMS	-23.7	20,020±90	24,230-23,590	BC 22,280-21,640	23,910±320	Rw	II
Airport	63.18	61.88	Beta-195936	shell	AMS	-0.7	>44,720					
Airport	78.64	77.34	Beta-192486	shell	AMS	-1.8	>42,880				Bg	

2.3.3. Amino acids racemization dating

Given that the AAR method is not a numerical method in isolation, it needs to be calibrated, mainly with radiometric dating methods. The racemization process model consists in the combination of diverse functions with different slopes. We establish a new age calculation algorithm to date samples up to ca. 30kyr with more accurate samples. The age calculation algorithms for different amino acids measured in ostracods are modified to improve correlation up to ca. 30kyr (Ortiz et al., 2004). The numerical age of the horizon was calculated using the aspartic acid and glutamic acid *D*/*L* ratios, and the algorithms of the age calculation for ostracods were established by Ortiz et al. (2004). The data from the Llobregat delta Complex were obtained using HPLC. They can be directly introduced into the aforementioned algorithms due to the similarities found between the aspartic acid and glutamic acid racemization ratios obtained with both methods (Torres et al., 2005). For the oldest samples (D/L Asp > 0.401 and D/L Glu > 0.140) the algorithms are (Ortiz et al., 2004):

- For aspartic acid (age in kyr B.P., eq. 4):

$$\sqrt{t} = -2.666 + 18.027\, Ln\left[\frac{1 + D/L}{1 - D/L}\right] \qquad \text{Eq. 4}$$

- For glutamic acid (age in kyr B.P., eq. 5):

$$t = -39.59 + 622.25\, Ln\left[\frac{1 + D/L}{1 - D/L}\right] \qquad \text{Eq 5}$$

- For younger samples (Middle-Upper Pleistocene), with *D*/*L* Asp < 0.401 and *D*/*L* Glu < 0.140, the algorithms are (Ortiz et al., 2004):

- For aspartic acid (age in kyr B.P., eq. 6):

$$\sqrt{t} = -3.586 + 19.745\, Ln\left[\frac{1 + D/L}{1 - D/L}\right] \qquad \text{Eq 6}$$

- For glutamic acid (age in kyr B.P., eq. 7):

$$\sqrt{t} = -3.186 + 58.972\, Ln\left[\frac{1 + D/L}{1 - D/L}\right] \qquad \text{Eq 7}$$

Because these latter algorithms were established using samples ranging from 4,5kyr B.P. to 170kyr B.P. and because the model of the racemization process (Goodfriend et al., 1988; Goodfriend, 1991) consists in the combination of diverse functions with different slopes (owing to the "non-linear" character of the racemization process), new algorithms are determined to calculate the age of Holocene up to ca. 30kyr samples. To this end, the amino acid racemization ratios of 9 samples (dated with radiometric methods) from the drill-hole cores of the Padul Basin (SPD), Banyoles Lake (BY) and the Llobregat Delta were used (table 2.4). For time zero, ostracods recovered from the Cabo de Gata saline (CGS-Andalusia, Spain) were also employed (Ortiz et al., 2004).

Table 2.4: Age and amino acid racemization ratios analyzed in ostracods of different location used in the algorithm of the age calculation. N: number of samples analysed on each statigraphic horizon.

Locality	Age (yr B.P.)	N	D/L Asp	D/L Glu	References
CGS	0	3	0.074±0.009	0.023±0.001	(Ortiz et al., 2004a,b)
Airport-49.11	6,045 ± 125	1	0.227	0.057	(this Chapter)
SPD-0198	6,782 ± 120	2	0.182±0.00	0.056±0.001	(Ortiz et al., 2004a,b)
SPD-0539	17,300 ± 500	7	0.255±0.013	0.058±0.007	(Ortiz et al., 2004b)
SPD-0710	24,998	7	0.283±0.014	0.074±0.008	
BY-4375	9,129	4	0.229±0.004	0.052±0.003	(Pérez-Obiol & Julià, 1996)
BY-7525	12,070	4	0.243±0.003	0.057±0.004	
BY-22475	20,268	4	0.271±0.019	0.053±0.008	
BY-29940	26,413	5	0.253±0.009	0.048±0.005	
BY-31530	27,722	3	0.289±0.013	0.057±0.002	

The Padul Basin (SPD) samples come from a 107-m long core (longitude 37º01´1´´N; latitude 3º36´7´´W), whose chronostratigraphy is shown in Ortiz et al. (2004). Two of these samples, SPD-0198 and SPD-0539, were dated by the radiocarbon method (table 2.4). The age of SPD-0710 was interpolated considering the ages of SPD-0539 (17300 ± 500 yr B.P. with ^{14}C) and SPD-0825 (30000 ± 1000 yr B.P. with U/Th). The Banyoles Lake samples (BY) come from a 33-m long core (longitude 42º72´N; latitude

2º45´E), whose chronostratigraphy (14C and U/Th) is reported in Pérez-Obiol et al. (1996).

In the SPD-0198, SPD-0539 and SPD-0710 samples from the Padul Basin, *Herpetocypris reptans* (Baird) was the only species determined, while in Banyoles, *Cyprideis torosa* (Jones) valves were picked. In the Airport 49.11 sample from the Llobregat Delta, a *Cushmanidea* valve was recovered and analysed (table 2.4). To select the best fit for the amino-age estimation algorithms, we compared the correlation coefficients (r) for various approaches (table 2.5). The relationship between the aspartic acid *D/L* ratio vs. square root of time (APK) was used because it provided the highest correlation coefficient.

Table 2.5: Correlation coefficients (r) between time and aspartic acid D/L ratios calculated in ostracod valves. The significant level (p) is also shown.

	D/L Asp	Ln (1+D/L Asp)/(1-D/L Asp)
Time	0.8278	0.8329
	p=0.003	p=0.003
Sqrt time	0.9419	0.9436
	p<0.001	p<0.001

The age calculation algorithm for aspartic acid (age in yr B.P.) is:

$$\sqrt{t} = -61.52 + 369.30\, Ln\left[\frac{1+D/L}{1-D/L}\right] \qquad r= 0.943,\ p< 0.001 \qquad \text{Eq. 8}$$

This equation (Eq. 8) can only be applied in samples with aspartic acid racemization ratios below that measured in BY-31530 D/L (Asp = 0.289±0.013).

However, given that the correlation coefficient with time or the square root of time is low (0.70) and given that the significance level is too high (0.02) for glutamic acid D/L ratios, this correlation cannot be considered to be useful for dating Holocene samples.

Numerical dating is obtained by introducing the D/L ratios into the algorithms of each amino acid. The age of a single horizon is the average of the numerical datings obtained for each amino acid D/L ratio measured in ostracods in that locality. The age uncertainty of a single horizon is the standard deviation of all the values obtained. For

samples younger than 30 kyr B.P., only the D/L aspartic acid ratios were considered for dating.

It should be borne in mind that ages obtained with amino acid racemization were calculated using ostracods from different genera. As the amino acid racemization method is genus-dependant, some uncertainty must be assumed for the mean ages calculated for each horizon.

Based on the calculation of amino acid racemization, we obtained ages between 6,713±2,950 and 9318± 1420 yr cal BP from the prodelta facies (in DS I, unit c). Samples from beach sand (in DS I, unit d, fig. 2.4) gave ages ranging between 4,533±2,642 to 16,662±3,825 yr cal BP (table 2.6). The upper palaeochannel, interpreted as beach gravel, at the base of Depositional Sequence I, in the eastern margin, yielded ages of 18,158±3,797 yr cal BP. The deposits below the upper palaeochannel (Depositional Sequence II) were dated at 104,861±4,230 (SOGIT-15 47.8), 26,385±1,311 (Airport 60.9), 70,210 ±3,621 cal BP (SPZ16-50.35) and 162,469±9349, 203,476±7,730, and 232,717±17,664 yr cal BP (SPZ-4 core, 48.6, 50.8 and 51.18m deep, respectively) (fig. 2.4, table 2.6).

Amino acid epimeritzation ratio was calibrated using the Airport-49.11 sample dated at 6,045±125 yr BP by the radiocarbon method (table 2.4). Figure 2.7 shows the relationship between the ^{14}C and the AAR. Even when the correlation between the AAR and ^{14}C methods is not perfect, the ages obtained from the AAR method allow dating of Pleistocene sediments with an error, which enables us to compare the ages with the eustatic sea level curve.

Table 2.6: Amino acid racemization results dated from ostracods in samples of Llobregat delta plain cores (fig. 2.4). Facies interpretation (fig. 2.3) and depositional sequence are also included. Genus (N): ostracod genre and number of valves analyzed in each stratigraphic horizon. Asp: aspartic acid; Glu: glutamic acid; BP: Before present. Nomenclature used in the Llobregat quaternary sediments: P (Prodelta); Bs (Beach sand); Bg (Beach gravel) and Rw (Multicolored fine-grained facies association). DS (Depositional Sequence)

Core	Depth (m)	M.B.S.L. (m)	Genus (N)	Sedimentary Enviroment	D/L Asp	D/L Glu	Age (yr BP)	Facies	DS
SRA-8	35.5	29.9	Hemicyprideis (3)	Neritic-Littoral	0.189±0.024	0.043±0.006	6,713± 2,950	P	I
SOGIT-15	28.98	27.78	Loxoconcha (5), *Cytheropteron* (3)	Circalittoral	0.210±0.009	0.053±0.001	9318± 1420		
Airport	48.92-48.98	46.92	Loxoconcha (3), *Bosquetina* (2),	Circalittoral	0.169±0.024 (0.205)	0.035±0.003 (0.038)	4,533± 2,642	Bs	
	49.06	46.98	Loxoconcha (3)	Circalittoral	0.232±0.004	0.083±0.003	12,933±711		
	49.11-49.19	47.11	Cushmanidea (1)	Brackishwater	0.227	0.057	12,013		
Pk2+537	15.3	8.6	Cushmanidea (9)	Brackishwater	0.250±0.024	0.060±0.002	16,662± 3,825		
SH	19.4	8.22	Cyprideis (5), *Cushmanidea* (2)	Brackishwater	0.258±0.017	0.078±0.011	18,158±3,797	Bg	
Airport	60.9	58.9	Cytheropteron (6)	Infralittoral	0.294±0.005	0.065±0.004	70,210 ±3,621	Rw	II
SOGIT-15	47.8	46.6	Costa (1)	Circalittoral	0.332	0.115	104,861± 4,230		
SPZ4	48.6	41.53	Costa (1)	Circalittoral	0.399	0.153	162,469± 9,349		
	50.8	43.73	Cytheropteron (5)	Infralittoral	0.432	0.199	203,476±7,730		
SPZ-16	50.35	45.69	Hemicyprideis (2)	Neritic-Littoral	0.468	0.191	222,724±21,862		
SPZ4	51.18	44.11	Cytheropteron (6), *Hemicyprideis* (2)	Infralittoral Littoral	0.459±0.022	0.215±0.003	232,717± 17,664		

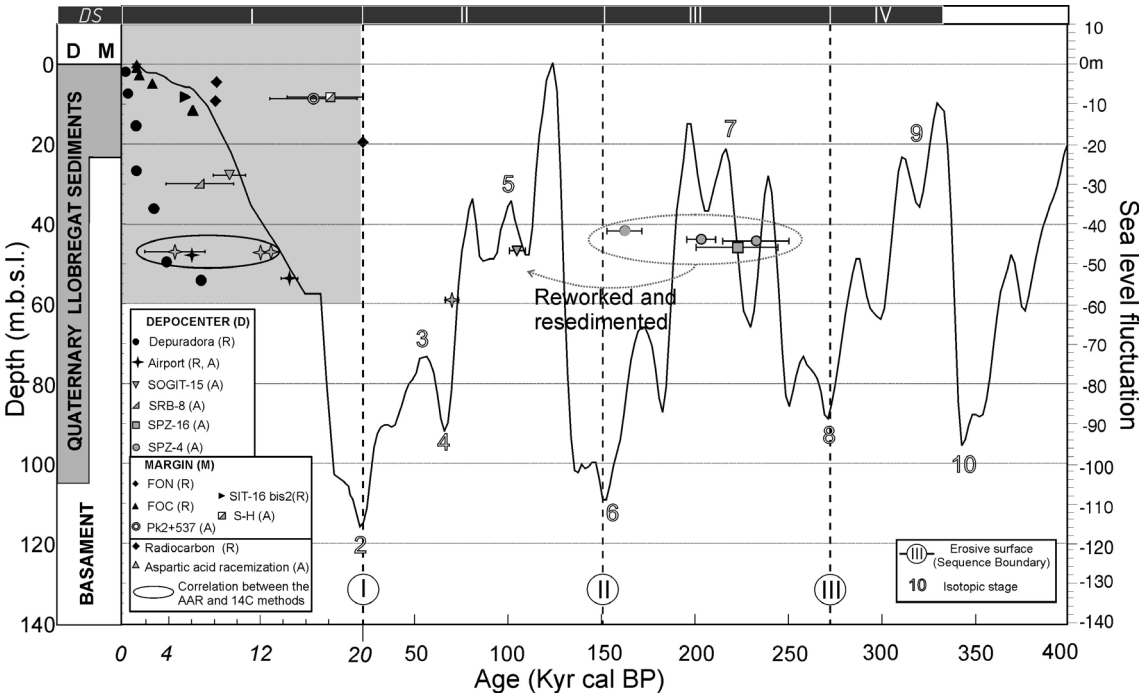

Figure 2.7: Age model for the Llobregat delta based on amino acid racemization, radiocarbon ages, sampling depth and sea level curve. We propose a correlation of the formation of the depositional sequences (DS) and major erosion surfaces (SB) described in the Llobregat delta complex with the trend of the sea-level curve and based on ages (see discussion in the text). Samples plotted in isotope stages 6 and 7 are mixed in the same stratigraphic unit with samples plotted in isotopic stage 5, suggesting reworking and resedimentation (see discussion in the text). The interpretation is supported by planktonic foraminiferal data (table II). Data in shaded area is used in figure 2.8 (0-20 kyr; 10 to 60 m.b.s.l.).

2.4. Geochronology Interpretation

2.4.1. Palaeogeographic evolution of the Holocene delta

a) General comments: controlling factors in the development of Holocene deltaic architecture

The controlling factors that determined the internal structure of Holocene deltaic progradation have been the subject of vigorous debates. Some authors have highlighted the importance of allocyclic processes (Swift et al., 1991; Fernandez-Salas et al., 2003) such as the deceleration of rising sea levels, the onset of high-frequency climatic changes (Cacho et al., 2001; Frigola et al., 2007; Goy et al., 2003; Jalut et al., 2000), and subtle changes in the sea-level (Somoza et al., 1997).

Other authors have focused on the dominant role of autocyclic processes such as channel avulsion in the alluvial plain and delta lobe switching (Trincardi et al. 2004). These processes are generally linked to fluctuations in sediment supply due to human (Correggiari et al., 2005; Liquete et al., 2004) or tectonic activity. Thus, pulses of deltaic progradation may be favored by an increase in sediment supply caused by deforestation, aridity, frequent stream-floods, and cold events, resulting in falling sea-levels. In contrast, a decrease in sediment supply allied to a fall in the hydraulic gradient during warm periods favored channel switching on the delta plain and the rapid abandonment of the main delta lobes (Somoza et al., 1997).

b) Controlling factors in the development of Llobregat Holocene deltaic architecture

In this section we consider the evolution of the Holocene delta, the sedimentary column that overlies the gravels and conglomerates deposited during the last glacial maximum represented by Depositional Sequence I (fig. 2.2). The deposition of the postglacial deposits as well as the distribution of the facies is controlled by the accommodation space available. This space is a function of the basement-Pleistocene palaeorelief and the position of the sea level.

These deposits have the oldest age at 14,565±715 yr cal BP. Comparison between depth and age (table 2.7) shows that the sedimentation rate in the center of the delta is 4.86 mm/yr during 6,815 ±165 to 1,170 ±100 yr cal BP and 0.67 mm/yr during 14,565 ±715 to 6,045 ±125 yr cal BP). Along the margin, the sedimentation rate was 2.3 mm/yr during the interval between 6,095±105 - 1,180±120 yr cal BP. figure 2.8 shows the data together with lines representing constant sedimentation rates of 1, 3, 5, 12 and 25 mm/yr for better visualization. figure 2.9 shows the sediment accumulation rate (including age error) vs. geological time as well as records of human activity in the study area (table 2.7). figure 2.9 is consistent with fig. 2.8 and emphasizes three phases of sedimentation rate in the center of the delta: during approximately 4000 yr cal BP, 1450 to 840 yr cal BP (VI-X centuries AD) and since 250 yr cal BP (XVIII century AD) (fig. 2.9). The relationship between the sedimentation rates and the evolution of the delta is dicussed below.

The sediments immediately above the gravels and conglomerates consist of shales and siltstones interpreted as swamp and marsh deposits and are capped by sands interpreted as beach barrier (figs. 2.2 and 2.3). The interpretation is based on the fauna and sedimentary lithologies and textures (table 2.8) and suggests that the coarsening upward succession is a retrogadational parasequence representing the transgressive deposits of the Holocene, which is consistent with the slow sedimentation rates and the reworking of fauna and sediments. Deposition of this unit occurred between 15,000 and 6,000 yr BP and forms a discontinuous deposit ranging from depths of 55 m in the depocenter (center of the delta) to 18 m along the margins (fig. 2.11). The beach barrier deposits, when present, are overlain by deeper water shales and siltstone indicating flooding of nearshore environments. These results are similar to other studies in the western Mediterranean (Boyer et al., 2005; Checa et al., 1988; Chiocci et al., 1997; Fernandez-Salas et al., 2003; Goy et al., 2003; Lario et al., 2002; Medialdea et al., 1986 and 1989; Somoza et al., 1998; Stanley et al., 1994; Vella et al., 2005; Zazo et al., 1996), which indicate a period a rapid increase in accommodation and slowing down at 6.9kyr BP (Fernandez-Salas et al.; 2003; Somoza et al., 1998; Zazo et al., 1996). It should be noted that the increase in floods and sediment supply during the Younger Dryas (10855-10230 yr cal BP) documented in the Llobregat river (Thorndycraft et al., 2006) is not recorded in the cores studied.

Table 2.7: Sedimentation rates obtained from dating of postglacial deposits cores from airport, depuradora and FOC in the Llobregat delta. The sedimentation rates are based on a best fit with age (mean cal BP) versus-depth (table 2.3). The maximum and minimum ages indicate the time interval for which every sedimentation rate applies. The grey area compares the sedimentation rates in the depocenter and the margin for the same time range. Results are plotted in figure 2.9. (*) meter below sea level.

Situation	Core	Depth range (m)* (d2-d1)	Bottom age (yr cal BP) t2±ξ2	Top age (yr cal BP) t1±ξ1	Sedimentation rate (mm/yr) sr (eq. 1)	Minimum error (εmin, eq. 3)	Maximum error (εmax, eq. 2)
Depocenter	depuradora	(7.30-1.90)	425 ±105	215 ±215	**25.71**	**10.19**	**+ ∞**
		(15.40-7.30)	1110 ±160	425 ±105	**11.82**	**8.53**	**19.28**
		(26.65-15.40)	1170 ±100	1110 ±160	**187.5**	**35.16**	**+ ∞**
		(36.20-26.65)	2610 ±150	1170 ±100	**6.63**	**5.65**	**8.02**
		(49.50-26.65)	3775 ±125	2610 ±150	**11.42**	**9.23**	**14.94**
		(54.10-49.50)	6815 ±165	3775 ±125	**1.51**	**1.38**	**1.67**
		(54.10-26.65)	6815 ±165	1170 ±100	**4.86**	**4.65**	**5.10**
	airport	(53.56-47.31)	14565 ±715	6045 ±125	**0.67**	**0.614**	**0.75**
Margin	FOC	(11.5-0.2)	6095±105	1180±120	**2.3**	**2.2**	**2.4**

The Llobregat Holocene Delta evolution and their controls are summarized in figures 2.9 and 2.10.

Reworked foraminifers are abundant in the lowest part of the transgressive deposits interpreted as a beach gravels and sand. Freshwater and brackish species are abundant above, interpreted as a swamp, back-barrier facies, whereas foraminifers from upper transgressive sediments were interpreted as a beach barrier. During this time the shoreline was located close to the palaeorelief (fig 2.10a and 2.10b). These patterns have been interpreted to reflect landward migration of barrier–lagoon–estuary systems during transgression, followed by extensive delta progradation during the subsequent sea-level highstand (Amorosi et al., 2004). The maximum flooding occurred during 6800 to 6000yr cal BP (fig. 2.11).

The first human activity at the Llobregat river head (Pyrenees, North Catalonia) was detected during 7000 and 6300yr cal BP and expanded as grazing after 4000yr cal BP (Pèlachs, 2004). Pollen analyses and archaeological sites close to Llobregat delta demonstrated that the first human activities began in the Neolithic (7600 to 7400 yr cal BP) (Burjachs et al., 1995; Jalut et al., 2000; Riera, 1994a). Nevertheless, the Mid Holocene fluvial environment indicated low energy fluvial systems that coincided with a Holocene Climate Optimum and reflected a sedimentary environmental stability with low sediment supply (Thorndycraft et al., 2006a).

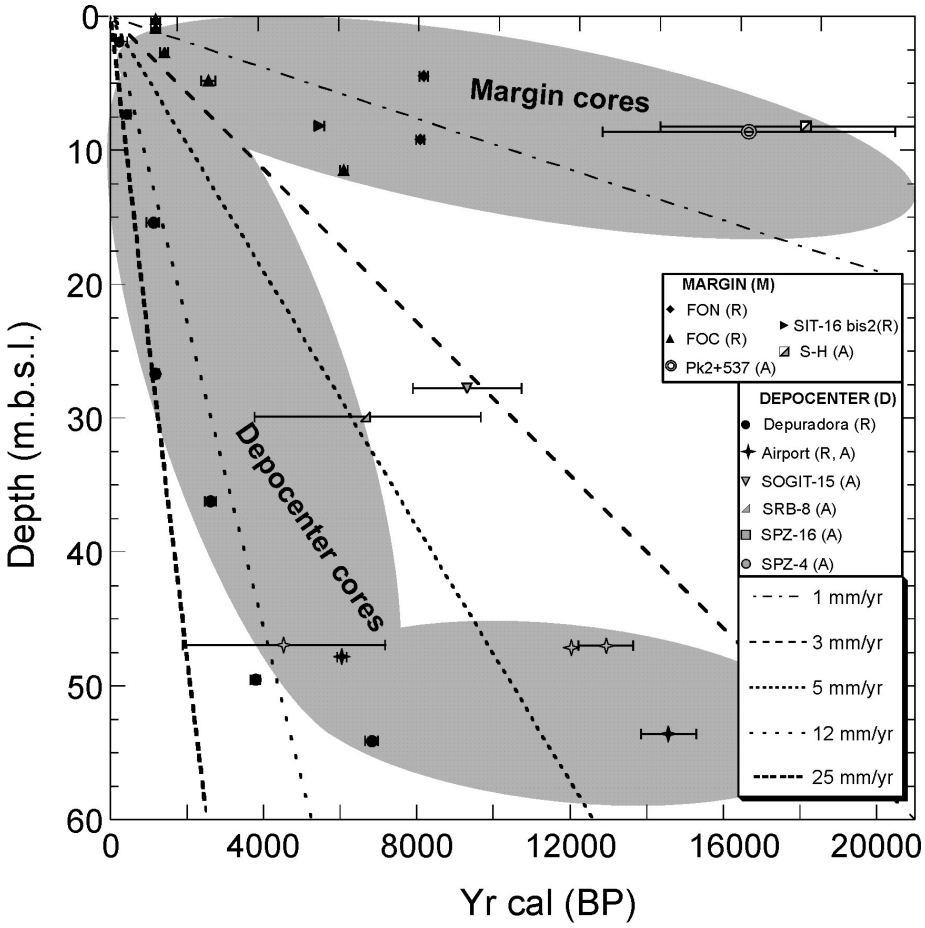

Figure 2.8: Relationship of sample depth (m.b.s.l.) and ages (mean yr Cal BP) from radiocarbon and aspartic acid racemization dating (table 2.3 and 2.6), of postglacial deposits. Dashed lines represent sedimentation rates of 1, 3, 5, 12 and 25mm/yr for better visualization. Data are grouped in cores from the depocenter and the margin of the Llobregat delta.

At 5300-4200yr cal BP, the present Mediterranean climate was established in the proximity of Barcelona (Jalut et al., 2000). The Llobregat delta pollen records revealed significant changes in vegetation at 5200 yr cal BP (Riera, 1994a), which coincided with the Atlantic to Subboreal pollen transit. This is marked by an increase in aridity (Jalut et al., 2000; Thorndycraft et al., 2006a) and by a cold event detected at 4000 yr BP (approx. 4200 cal yr BP) (Frigola et al., 2007) (fig. 2.9). Archaeological studies undertaken at the Mines de Can Tintorer in the western Llobregat delta plain (table 2.1) reported considerable human activity during the Neolithic epoch, shaping the land use of the Garraf slope (Riera, 1994a). Human activity and dry/cold conditions gave rise to a more detritical input in the Llobregat delta from 4500 to 4000yr cal BP (BC 2050), triggered a pulse of deltaic progradation, which is in line with figures 2.9 and 2.10c. Deep water facies (offshore) and shallow facies (lower shorefaces) were deposited in

the center of the delta, whereas littoral facies were deposited close to the palaeo-cliff along the margin.

Radiocarbon data close to the apex at 3185±29yr BP (St Boi, table 2.1) lend support to a phase stabilization during 3000-4000yr cal BP. Before Iberian-Roman times (VI century BC- V centuries AD), settlements were distributed along the ridge of the hill at Montjuïc in the eastern Llobregat margin. During Iberian-Roman times, the settlements occupied new areas on the southern slope of the hill at Montjuïc. This confirms the short distance between the settlements and the shoreline (fig. 2.1) (Izquierdo et al., 1998; Riera et al., 1994b).The lagoon-beach barrier system in the eastern margin was preserved and was used as a harbor, known as Port harbor, in Iberian times (V century BC, approx 2350 yr BP) (fig. 2.10d). Despite being a harbor, Port harbor had a shallow depth (less of 30 m) because of the sediment supply from the Montjuic hill and the Collserola Mountain range. This lagoon-beach barrier system was filled during Roman times (I century BC, approx 2050yr BP), with the result that the Port harbor activities were shifted to the Les Sorres harbor anchorage (western margin) (Izquierdo et al., 1998; Raurich et al., 1992) (fig. 2.9d).

Archaeological documents demonstrate that the Les Sorres anchorage disappeared as early as the V century AD, (approx 1550yr BP) because the anchorage was filled with sediment from the Llobregat basin (Izquierdo et al., 1998; Raurich et al., 1992). The foregoing account is supported by the sedimentation rate analysis from the cores in the center of the delta, which provides evidence of this progradation pulse (fig. 2.9).

The analysis of the pollen diagram carried out in the Besos delta (NE of the Llobregat delta, fig. 2.1), in the Catalan littoral plains (Riera et al., 1994a) and in the Pyrenees (Pèlachs, 2004) detected ash dated to 1300yr cal BP (VII-VIII centuries AD) because of intensive economic activity in the area (Riera et al., 1994b). According to Riera et al. (1994b), the resulting deforestation caused the instability of the southern slope of the Montjuïc hill (fig. 2.1). These authors found pre-Iberian to Roman remains in alluvial facies in the cores located in the eastern Llobregat margin. However, the absence of medieval pottery confirms the occurrence of sedimentation between Roman times and before the start of the Medieval period. The FOC core (FOC-9.5, fig. 2.4)

recorded sands with some pebbles in marsh facies overlying sand and peat dated at 1510-1300yr cal BP (AD 440-650) in the eastern margin of the delta plain (table 2.3). The sedimentology, archaeological and the radiocarbon data are in line with the marsh filled in Roman times.

This human impact in addition to an increase in aridity (during 1300-750yr cal BP, (Jalut et al., 2000) and a new cold event (at 1600yr BP , Frigola et al., 2007) triggered a new progradational pulse due to a large detritical input. Studies on the agricultural structure and road network from VII to X centuries AD lend further support to these physical changes on the delta plain (Palet et al., 1997; Riera et al., 1994b). The large detritical input is also supported by the sedimentation rate peak detected in the Llobregat cores between 1450 and 840 yr cal BP (VI-X centuries AD) in the depocenter (fig. 2.9).

A phase of shoreline stabilization commenced around 1300yr cal BP (VII-VIII centuries AD) in the eastern margin from marsh facies dated in the FOC core (FOC- 7.7 to 6.6, table 2.3, fig. 2.4) (Garrigosa; Gimenez et al., 1994; Riera et al., 1994b). Figure 2.10d shows the position of the shoreline during 1300-1200yr cal BP.

Late Holocene shorelines were reconstructed from historical maps (Izquierdo et al., 1998; Marques, 1984; Riera et al., 1994b). In the Llobregat delta the high magnitude palaeofloods occurred during 853-554yr cal BP (AD 1097-1396) (Thorndycraft et al., 2006c). Nevertheless, sedimentation rate analyses of cores in the center of the delta do not record an increase in sediment supply and indicate low sedimentation rates during this period. This suggests avulsions and a sudden abandonment of the lobes in the center of the delta, switching to the south-western margin during X century AD (fig. 2.10e). The agricultural structure map of the Medieval period displays these deltaic lobe avulsions on the delta plain at the end of X century AD (fig. 2.10e) (Palet et al., 1997). Despite the fact that the Les Sorres anchorage disappeared due to the position of the new lobes, the Mutrassa marsh was navigable between the V and XIV centuries (figs. 2.1 and 2.10d) (Izquierdo et al., 1998; Raurich et al., 1992). Archaeological remains in the western margin also confirm these observations (fig. 2.1 and table 2.1).

Subsequently, the reduction in flood events during the XIV-XV centuries (Thorndycraft et al., 2006b) accounts for the low sediment accumulation and

distribution along the shoreline due to long-shore currents (fig. 2.10e). This sedimentation process was deduced by Palet et al. (1997) from agricultural structure map and by Marques (1984). This sedimentation process is also confirmed by facies distribution in this area (fig. 2.10e).

Historical and pollen studies show that after the Lower Medieval Crisis the Llobregat basin underwent considerable modification in the XVIII century AD (Pèlachs, 2004; Riera et al., 2004). The economic recovery together with an increase in the flood frequency during the AD 1580-1620, 1760-1800, 1830-1870 coinciding with the Little Ice age was recorded in the Llobregat (NE Spain) and Western Mediterranean rivers (Barriendos et al., 1998; Llasat et al., 2005; Thorndycraft et al., 2006a). This increase in flood frequency probably resulted in a high sediment discharge and avulsion in the Llobregat main distributary channel (fig. 2.10f). These observations are in line with the second peak in the sediment rate curve observed in fig. 2.9 in the Llobregat delta.

c) In comparison with other Mediterranean deltas

In the Llobregat delta, the rapid rise in the sea-level between 15,000 and 6900yr B.P triggered the rapid migration of beach barrier–lagoon–estuary systems, forming retrogradational-aggradational stacking patterns. The top of the transgressive deposits is interpreted as the Holocene 4th-order MFS dated at 6980-6650yr cal BP (table 2.3). Peats from the Ebro delta yielded similar results (Somoza et al., 1998).

After the transgressive period, deceleration of the sea level rise and changes in sediment supply played a major role in the emplacement of the Llobregat highstand deposits, triggering progradation. Progradational deltaic lobes could be associated with 5th-order oscillations (Dabrio et al., 2000; Somoza et al., 1998). However, higher frequency periodicities on a millenial to submillenial scale were not recognised.

The first progradational pulse detected in the Llobregat delta occurred after 4500-4000yr BP. This was caused by an increase in aridity, a cold event and low to moderate human activity. An early period of deltaic progradation has also been registered in the Ebro delta between 4400 to 3600yr BP and in the Rhône delta between 4000 and 2400yr BP (Somoza et al., 1998; Vella et al., 2005).

A large progradation in the northeastern Llobregat delta during 1500 and 840yr BP (V-X centuries AD) has been assumed on the basis of the archaeological remains and historical documents. The archaeological remains and historical documents provide evidence of the change of site of the two old harbors in the Llobregat delta during Roman times (Izquierdo et al., 1998; Raurich et al., 1992). Moreover, historical documents corroborate the evolution of the agricultural structure in the delta plain from VII to X centuries AD (Palet et al., 1997). This second progradational pulse was caused by the increase in sediment supply due to deforestation, aridity and a cold event. This increase in sediment supply was recorded in cores from the center of the Llobregat delta. This second progradational phase has also been detected in the Po and Tiber deltas during 1800–1300yr BP (Belloti et al., 1995; Stefani et al., 2005).

Avulsion and a sudden delta lobe switch to the southwestern margin of the Llobregat delta occurred during the X century AD. Subsequently, a reduction in flood events during the XIV-XV centuries AD resulted in sediment redistribution along the shoreline. Changes in sediment supply in the XVIII century AD due to increased palaeflood frequency and anthropic pressure probably caused the migration of the Llobregat tributary channel observed in historical maps (Izquierdo et al., 1998). These phases of increased flood frequency appear to coincide with the Medieval Warm Period (IX–XIV centuries AD) and the Little Ice Age (XIV-XIX centuries AD) (Thorndycraft et al., 2006a). A sea-level fall during the Little Ice Age together with the increase in palaefloods triggered a large sediment discharge, aggradation of the floodplain, development of the deltaic lobes and progradation of the coastline (Boyer et al., 2005; Thorndycraft et al., 2006a). This last progradational phase has also been reported in most Mediterranean deltas (Amorosi et al., 2001; Boyer et al., 2005; Cattaneo et al., 2003; Goy et al., 1996; Somoza et al., 1998).

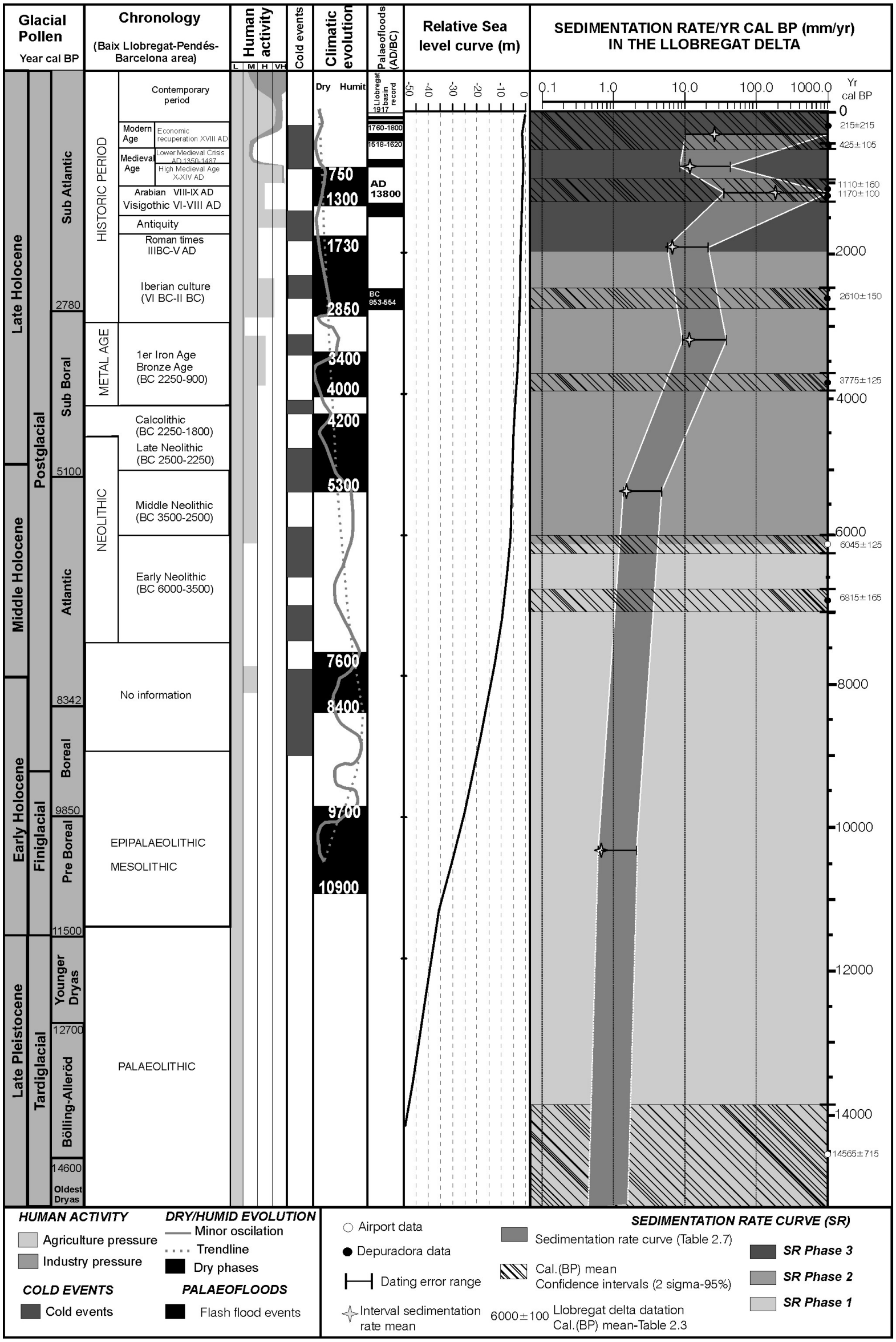

Figure 2.9: Variation in the sedimentation rates in the Llobregat delta in table 2.7 and their correlation to: pollen-glacial chronology (Costa et al.,1998); Barcelona chronology and anthropic pressure variation (Riera, 1994a i b; Riera and Esteban, 1994; Riera and Palet, 1994b Pèlachs, 2004); climatic events (Burjachs et al., 1995; Jalut et al., 2000a; Frigola et al., 2007a; Riera et al.,2004); major palaeoflood events (Barriendos et al., 1998; Llasat et al., 2005; Thorndycraft et al., 2006); and global sea level curve (Labeyrie, 1987). It should be noted that the sedimentation rate is plotted using a logarithmic scale, and the time scale (in y-axis) includes the ages (Cal BP, with the 2σ confidence interval) from the "Depuradora" and Airport cores (tables 2.3 and 2.7). The definition of the three major sedimentation rate phases is discussed in the text.

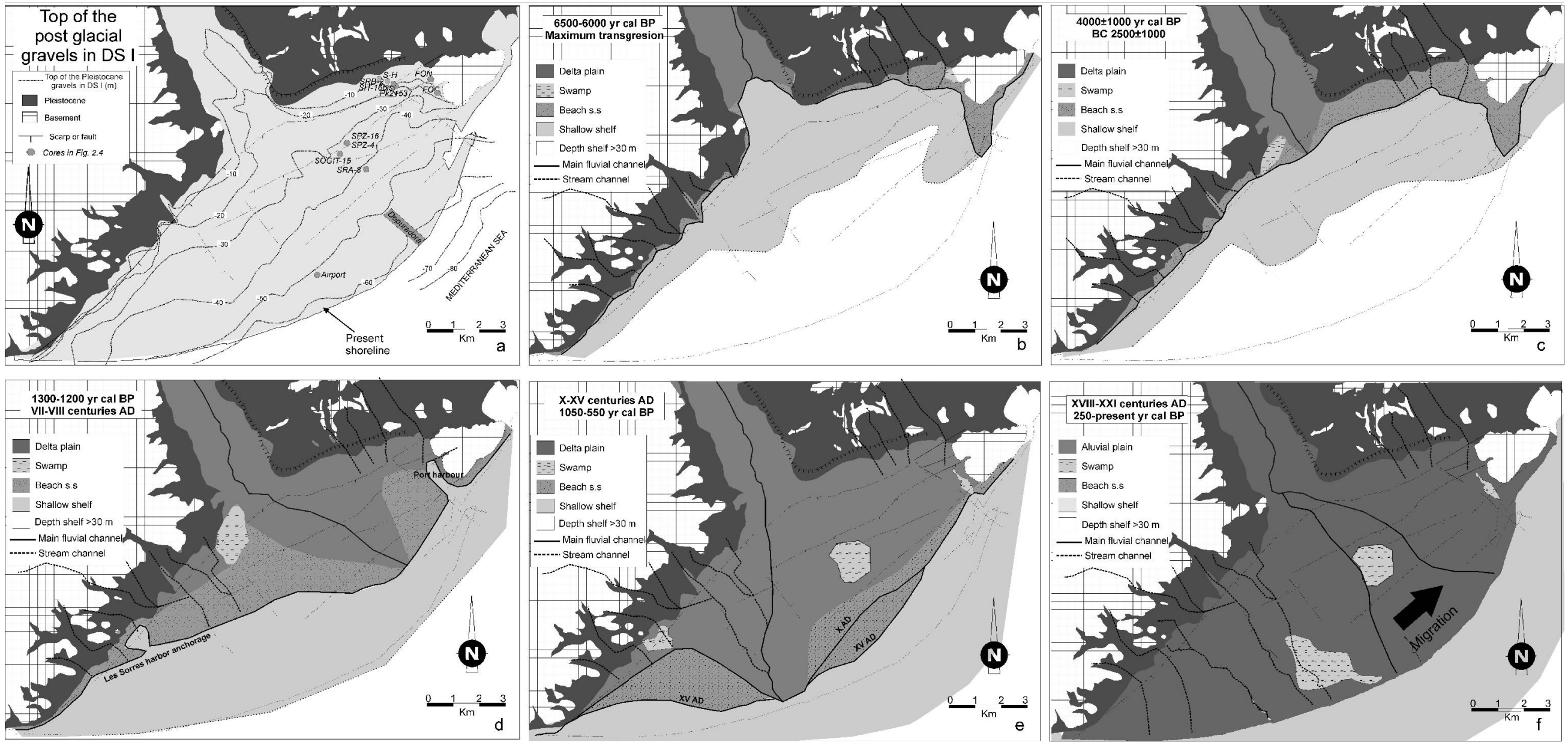

Figure 2.10: Llobregat Delta coastal progradation and fluvial network evolution over highstand (HST) times, 6500 cal yr BP to the present. Map 10a shows the palaeorelief of the basement (this includes the postglacial gravels, Pleistocene deltas and prepPleistocene) or the base of the highstand deposits. Dark grey zones depict fresh and brackish water regions, light areas represent salt water marshes. Maps since X century AD (10e and 10f) are modified from Palet et al. (1997).

2.4.2. Pleistocene delta formation and chronology

a) Delta formation

The onshore Llobregat Pleistocene succession consists of three erosional bases interpreted as a sequence boundary (SB), with characteristics similar to those observed in other Mediterranean delta plains (Aguzzi et al., 2006; Amorosi et al., 1999; Amorosi et al., 2004; Lucchi et al., 2006; Vella et al., 2005). Facies architecture above the erosional surface includes lowstand and transgressive stacking patterns of fluvial channel (Fc, fig. 2.3) and beach gravel facies (Bg, fig. 2.3) (Chapter 3). Transgressive deposits are generally preserved within the channels. Resedimentation (due to mixing of marine and brackish water foraminifers) and reworking (due to mixing of foraminifers from different ages) were identified in the palaeochannel transgressive deposits in the Depositional Sequences I and II (Amorosi et al., 2004).

The other important surfaces are the Maximum flooding surface (mfs) overlying the transgressive deposits. These surfaces are underlain by a delta succession interpreted as the actual HST delta in Depositional Sequence I (discussed in section 2.4.1) and by fine sediments interpreted as continental and marine facies (Rw, fig. 2.3) in Depositional Sequences II and III. Rw facies are truncated by the consecutive sequence boundary surface (Chapter 3).

Vertical foraminiferal distributions within the Rw facies in DS II shows high resedimented and reworked benthonic foraminiferal content that decreases with depth (table 2.8, fig. 2.6). Rw sediments are interpreted as a Highstand systems tract (HST) and FSST (Falling stages). According to seismic profiles, FSST deposits display a thinning wedge towards the delta plain (Chapter 3). Thus, it may be assumed that Rw may be represented by HST deposits, and FSST of less thickness. In line with Amorosi et al., (2004), we interpreted the FSST as dominated by alluvial plain sedimentation (with paludal/lagoonal episodes), which is markedly discontinuous. By contrast, the HST are dominated by beach ridges and prodelta. The high resedimented and reworked foraminifers in HST deposits could be attributed to the high energy environment (washover and beach ridges facies, table 2.8), and to the sediment sources from the Miocene (Montjuic) and Pliocence (Llobregat delta plain basement and lower

river valley) sediments. The channel migration could cause erosion of older deposits resulting in the introduction of reworked foraminifers. These hypotheses agree with the observations made in the present HST (Cearreta et al., 2000) and pleistocene HST deposits (Amorosi et al., 2004).

The formation of the FSST deposits was due to fluvial cannibalization of the earlier transgressive, regressive and basement deposits during the sea level fall. In the FSST sediments we observed ostracods and foraminifers, which are resedimented and reworked even in flood plain facies. Forced regressive deposits with multiple reworking and redeposition have been observed in delta plains and outcrops (Amorosi et al., 2004; Cantalamessa et al., 2004; Massari et al., 1999) and shelves in the Mediterranean (Chiocci, 2000; Hernández-Molina et al., 2000b; Lobo et al., 2004b; Tesson et al., 2000; Trincardi and Correggiari, 2000).

LOCATION	CORES		LITHOFACIES	DATING: Radiocarbon	DATING: Amino acid racemization	TAPHONOMIC PROCESSES: Resedimented	TAPHONOMIC PROCESSES: Reworked	TAPHONOMIC PROCESSES: Broken	DIAGENETIC: Iron oxides	DIAGENETIC: Pyritization	TEMPERTAURE	ENVIROMENTAL INTERPRETATION: Marine: Prodelta	Marine: Beach ridges	Marine: Beach barrier	Brackishwater: Washover	Brackishwater: Lagoon	Brackishwater: Marsh	Freshwater: Flood plain	Freshwater: Swamp	FACIES UNIT	AGE (Forams)	DS-Fig 2.4
DEPOCENTER	SPZ-4	47.8	Gravels with fine matrix			■		■	■		Warm			■						Bg	?	I
		48.6	Yellow clays and silt		162469±9349	■			■							■					Q	II
		49.2	Fine sand with laminations			■	■	■	■						■							
		49.63				■									■							
		49.98	Yellow clays and silt			■		■							■							
		50.0	Silty sand			■		■							■							
		50.8	Sandy silt		203476±7730	■		■			?									Rw	Q	
		51.18*			232717±17664																?	
		51.59	Silty sand					■	■				■								Q	
		52	Sandy silt					■					■									
		52.44	Silty sand					■					■									
		52.8						■					■									
		58.4	Yellow silty clay, with dotted organic matter							■						■					Q	III ?
	Airport	48.92	Sandy silt		4533±2642	■					?			■						Bs	Q	I
		48.98				■								■								
		49				■								■								
		49.06*			12933±711																?	
		49.11		6170-5920	12013	■																
		54.86*	Silty sand with organic matter	15280-13850				■								■				M		
		60.9	Silt with lamination		70210 ±3621					■					■					Rw		II
		63.18*	Silty sand	<44720									■									
		65.68	Fine to medium sand			■		■		■	Warm											
		71.8	Red clays			■					?							■				
		78.6	Gravels with fine matrix	<42880			■		■		Warm			■						Bg		
		88.1	Red clays															■		Rw		III
		99.1	Yellow silt				■		■							■						
		103.5	Silty sand				■						■									IV ?
		105.2	Clays			■	■	■	■							■						
MARGIN	SRA-8	22.40	Silty clay						■		?								■	P	?	I
		35.5*	Silty sand		6713±2950							■										
	SPZ-16	50.3	Silty sand		222724±21862	■	■		■		Warm		■							Rw	Q	II
	SOGIT-15	45.35	Marls			■					?					■						
		47.8*	Sandy marls		104861±4230																?	
	Pk2+537	15.3	Grey fine sand		16662±3825	■								■						Bs		I
	FON	18*	Black silt	8200-7980						■								■		Sw	?	
		21.2	Black silt																			
	S-H	19.4	Yellow coarse to medium sand		18158±3797	■	■				?		■							Bg		
	SIT-16 bis2	15*	Gravels with fauna	5580-5320		■	■							■								
		17.0	Brown sandy silt			■	■	■													Q	

Table 2.8: Summary and analysis correlation of samples. Results include amino acid racemization, radiocarbon, foraminifers and sedimentology description. (*) Not foraminiferal identifications

b)Age model

We evaluated the results from foraminifers, numerical ages and sedimentology and compared them with the global sea level curves derived from isotopic data. This correlation provides a geochronological framework for the Pleistocene deposits.

The transgressive deposits in Depositional Sequence I give an age between 18158±3797yr BP to 5450± 130 (fig. 2.7 and table 2.8). These sediments indicate deposition during the last glacial maximum (MIS 2) and reworking during the sea level rise in MIS 1 (figs. 2.7 and 2.11). Rw facies in the Depositional Sequence II below the postglacial deposits (DSI) were dated in cores located very close to one another with similar stratigraphic columns (SPZ-4, SPZ-16 and SOGIT-15, fig. 2.11), yielding a range of 104861±4230 to 232717±17664 yr cal BP (table 2.8). Moreover, Rw sediments in the Airport core gave an age of 70210 ±3621 cal yr cal BP (fig. 2.11, table 2.8). When we compare the ages in a depth/time diagram with the sea level curve (fig. 2.7), we observe that the samples from the Airport and SOGIT-15 cores indicate a deposition during the interglacial period of MIS 5 (fig. 2.7). However, the ages from SPZ-4 and SPZ-16 cores are older than those of the Airport and SOGIT-15 ages since they were deposited during the interglacial period of MIS 7. These ages represent controversial results given that they are derived from the same stratigraphic unit. Further palaeontological analyses agree with the lithofacies description of the cores. The presence of the foraminiferal indicators of warm temperature in the Rw samples indicates an interglacial period (table 2.8) in contrast to the SOGIT-15, SPZ4 and SPZ-16 samples deposited during glacial period in FSST (fig. 2.7). Most of these SPZ-4 and SPZ-16 samples present a considerable degree of reworked and resedimented fauna with numerous broken shells refilled with sediment, and often oxidized. Most of the ostracod species dated by amino acid racemization were deposited in different sedimentary environments from circalittoral to brackishwater (table 2.8). These environments are not consistent with the foraminifers environments. According to the "delta formation" section, the high degree of sediment remobilization in the Rw facies indicate deposition during highstand interglacial periods and redeposition during episodic sea-level falls in glacial periods (fig. 2.6). Therefore, the SPZ-16 and SPZ-4 ages are indicative of a deposition during MIS 7 sea-level fall and of a subsequent

resedimentation during MIS 5. Similar observations have been made in deposits formed during sea level falls in other coastal systems (Murray-Wallace et al., 1996; Wehmiller, 1995).

Despite the absence of ages for Depositional Sequence III, we consider similar chronostratigraphic patterns discussed in Depositional Sequences I and II, taking into account the micropalaeontology analysis made in Despositional Sequence III. Thus, Depositional Sequence III was deposited during the earlier eustatic cycle (MIS 8 to MIS 6), with the same sedimentation mechanism discussed in Depositional Sequence II. Other depositional sequences may be observed in sediments in the Airport core (figs. 2.4 and 2.11). These deposits may be correlated with deltas offshore corresponding to Depositional Sequence IV (Chapter 3).

The integration of radiocarbon and amino acid racemitzation ages and foraminiferal analyses lend support to the circa 100Kyr glacio-eustatic cycles, where the erosional surfaces (SB) correlate with significant sea-level falls (MIS 2, 6 and 8).

These results agree with the Travertine dating obtained from the middle River Llobregat fluvial terraces accumulated during high sea level periods MIS 5e and MIS 9, with a 100 Kyr cyclicity (Luque et al., 2007). Studies on the Mediterranean sea have also reported circa 100Kyr sea-level cycles (Chiocci et al., 1997; Chiocci, 2000; Rabineau et al., 2005; Trincardi and Correggiari, 2000).

The definition of the basement based on foraminiferal data is problematic because Miocene fossils appear reworked in Pliocene samples and because both Miocene and Pliocene fossils are reworked in Quaternary samples. Using a muti-approach strategy (fauna, taphonomy, age dates, sedimentology,…) we interpreted the SPZ-4 63.8, 68.2, Airport-118.9, 126.4, 135.45, SRB 2-18.2 and I2+580-31 samples, which are Pliocene in age (tables 2.2 a, b, and c).

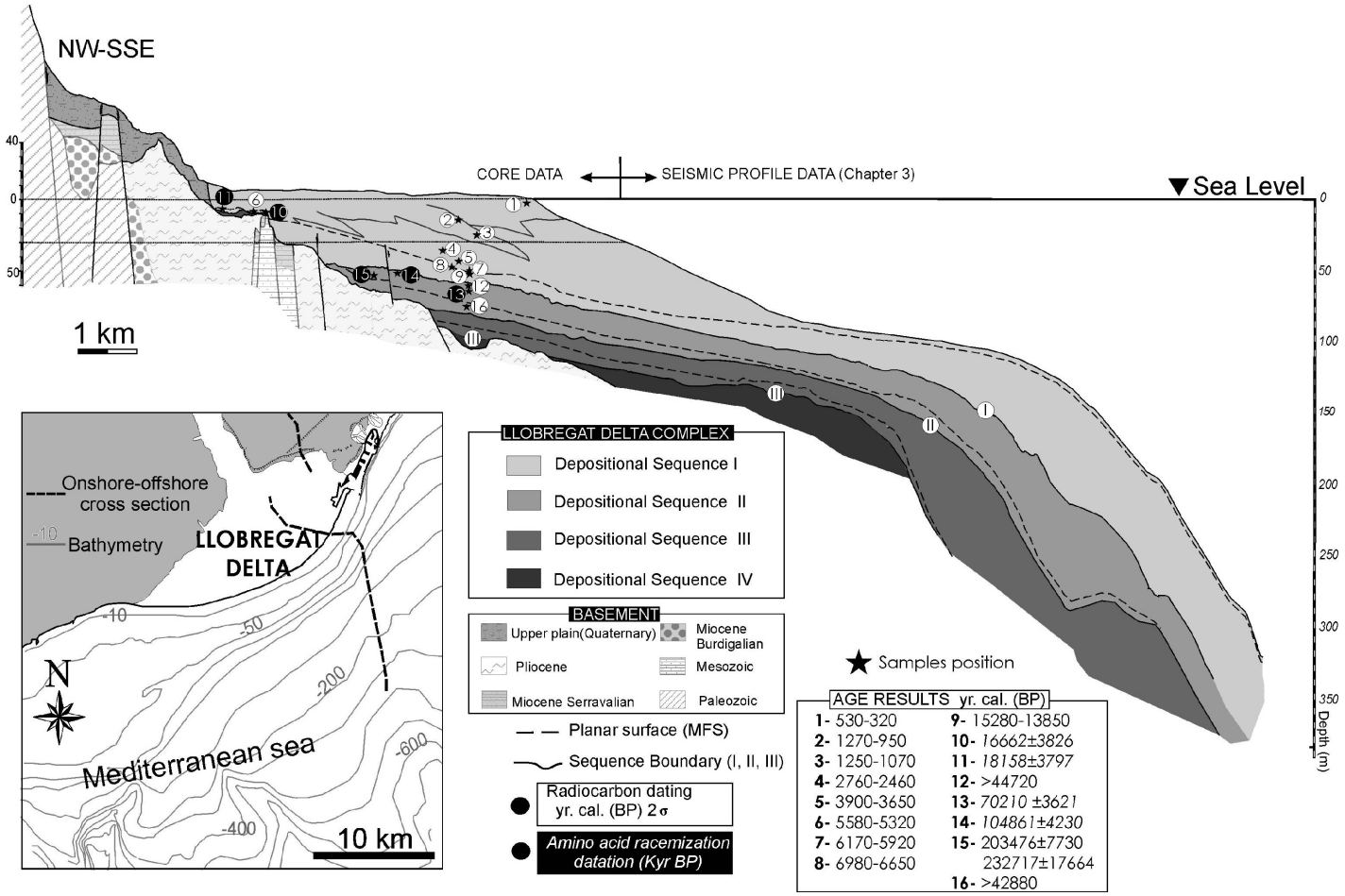

Figure 2.11: Onshore-offshore depositional sequence correlation. Ages discussed in the text are plotted in the figure. Erosive and planar surfaces are also displayed. The cross section location is on the right.

2.5. Conclusions

Multidisciplinary analysis of cores from the Llobregat delta plain offers a coherent picture of the Late Quaternary evolution in the Mediterranean and provides a geochronological framework for the onshore-offshore Pleistocene Llobregat delta.

a) Holocene palaeogeographic delta evolution

Cyclic and random factors control the internal architecture of the Llobregat delta. The changes in the relative sea-level and the basement palaeorelief controlled the accommodation space in the Llobregat delta basin. Human activity in the Llobregat river basin together with palaeoflood frequency, humid/dry periods and cold events accounted for the variations in sediment supply. Based on radiocarbon results and facies analysis three phases of sedimentation rate were observed:

1) From 14586 to 6045yr cal BP a low sedimention rate was controlled by the high accommodation space due to the sea level rise, which favored a retrogradation stacking pattern.

2) From 6055 to 1900yr cal BP an increase in the sedimentation rate showed a marked increase from 4500yr cal BP induced by a slow sea level rise and by large inputs of sediment supply, which favored the deltaic progradation.

3) From 1900 to 215yr cal BP a marked variation in the sedimentation rate caused by the avulsion of the river alluvial plain, resulting in the sudden abandonment of major river branches and in a delta lobe switch due to palaeofloods and human activity.

b) Pleistocene delta geochronology

Detailed studies on the sedimentology, age and micropalaeontology (foraminifers and ostracods) show a vertical cyclic pattern of facies, including a considerable degree of reworked and resedimented fauna. The ages and these reworked and resedimented foraminifers confirm the high energy in the Highstand environment and in the fluvial cannibalization during the sea level fall, facilitating

erosion of the previous deposits and their redeposition. Thereafter, these sediments were eroded and resedimented during the sea level rise.

The Llobregat architecture consists of four Depositional Sequences bounded by a minimum of three erosional surfaces described in the onshore-offshore area. These three erosional surfaces were governed by circa 100Kyr glacio-eustatic cycles and are regarded as the major glacial/interglacial sea-level fluctuations. In particular, glacial intervals are characterized by continental facies formed during sea level falls, and by three fluvial facies formed during low sea levels. The interglacial intervals are made up of fluvial facies that were eroded and resedimented, forming beach facies during the sea level rise. These intervals were also characterized by prodelta and delta front facies during highstand sea levels.